geosciences

MDPI

Article

Evolution of Coastal Subarctic Lakes in the Context of Climatic and Geological Changes and Human Occupation (North-Central Labrador, Canada)

Camille Latourelle-Vigeant *, Reinhard Pienitz and Najat Bhiry

Département de Géographie and Centre D'études Nordiques, Université Laval, Québec, QC G1V 0A6, Canada
* Correspondence: camille.latourelle-vigeant.1@ulaval.ca

Abstract: Climate fluctuations and landscape evolution, with their associated impacts on northern coastal ecosystems, likely influenced human populations of Nunatsiavut who have inhabited the region for nearly 7000 years. As part of an interdisciplinary research initiative within the Nain Archipelago on the subarctic coast of Labrador, this project sought to reconstruct the postglacial palaeoclimatic and palaeoenvironmental variability of Dog Island and document its impacts on the evolution of lakes located in the vicinity of significant archaeological sites. To address these questions, we analysed physical, geochemical, and biological indicators preserved in sediment cores of two lakes. Results from Oakes Bay West Lake revealed gradual acidification since ca. 4900 cal. yr BP, coherent with terrestrial vegetation development and/or neoglacial cooling, interrupted by periods of milder climatic conditions (ca. 4900–3640 cal. yr BP and ca. 1520 cal. yr BP—present) that favoured large sediment inputs. Evilik Lake revealed the classic sequence of isolation of the basin in three major phases in response to glacio-isostatic rebound. These complementary results allowed for the development of a local palaeoenvironmental framework that contributes to a better understanding of how landscape evolution and climate have influenced human societies through site availability and proximity to marine resources, and how, in turn, they impacted their immediate environment through activities, such as wood harvesting and its associated effects on nutrients and lake sediment inputs.

Keywords: palaeogeography; palaeolimnology; human–environment relationship; environmental archaeology; Nunatsiavut; Labrador; climate change

Citation: Latourelle-Vigeant, C.; Pienitz, R.; Bhiry, N. Evolution of Coastal Subarctic Lakes in the Context of Climatic and Geological Changes and Human Occupation (North-Central Labrador, Canada). *Geosciences* **2023**, *13*, 97. https://doi.org/10.3390/geosciences13040097

Academic Editors: Jesus Martinez-Frias and Tadeusz Marek Peryt

Received: 17 February 2023
Revised: 21 March 2023
Accepted: 22 March 2023
Published: 24 March 2023

1. Introduction

Contemporary climate warming occurred relatively late in Eastern Canada (late 20th century), particularly in Labrador, when compared to adjacent circumpolar regions (since 1850 AD) [1–3]. Accelerated temperature increases over recent decades raise important questions about the vulnerability and resilience of Arctic and subarctic coastal ecosystems, while posing serious social, cultural, and economic challenges for Labrador Inuit communities [4–7]. Specifically, rapid changes in northern environments have the potential to disrupt ecosystem services, leading to direct impacts on the availability, accessibility, and quality of food resources, as well as on landscape use and transmission of Inuit traditional environmental knowledge [8]. As such, Labrador's coastal landscapes are of particular interest with respect to the conservation of ecological and socio-cultural aspects of the Nunatsiavut territory [2].

The impacts of continued warming on the structure of the physical and biological environment are not uniform in time and space [1,9]. Labrador's coastal climate and ecosystems, influenced by many external natural factors and subject to anthropogenic pressures, are particularly vulnerable to changes in the dynamics of North Atlantic oceanic and atmospheric parameters [3,10,11]. In this context, a comprehensive understanding of the long-term effects of climate fluctuations on the region's terrestrial and aquatic ecosystems is essential to understand the extent of their natural variability, to identify

the underlying processes and factors that influence their dynamics, and to contextualize recent changes [1,9]. Palaeoecological studies offer the opportunity to anticipate potential responses of subarctic coastal environments to future climate change (ecological trajectories) and to estimate the extent of their impacts, past and future, on human communities [12].

1.1. Human Occupation in the Context of Environmental Change

Changes in Labrador's coastal landscapes, driven by palaeogeographic and palaeoenvironmental evolution, geophysical processes, and climatic fluctuations, are likely to have had a significant impact on human land use patterns, as well as subsistence activities, by altering site habitability and resource accessibility for communities [13,14].

A land of migrations, cultural transitions, and human occupation for over 7000 years, the subarctic coast of Labrador presents many opportunities to assess postglacial climate variability and its impacts on terrestrial and aquatic environments and human populations [4,5]. Nain and its archipelago, consisting of a multitude of islands off the north-central coast of Labrador, have historically been a preferred area for human settlements given their more favourable wind-protected climate and rich marine, terrestrial, and freshwater ecosystems, while the archaeological sites are among the most studied in Nunatsiavut [4].

The multiple cultures that successively inhabited the region, from the Maritime Archaic to Dorset, Thule, and Inuit, experienced and adapted to an array of different and unstable climatic conditions and to changes in their environment [13,15,16]. While Holocene climatic fluctuations have long been identified as a key determinant of cultural transitions and changes in subsistence activities and settlement patterns observed among human populations in Labrador [16–18], other archaeologists have highlighted the role of multiple socioeconomic, historical, and cultural factors [4]. For example, some researchers have suggested that the cold, unstable climatic period of the Little Ice Age (LIA) and its associated negative biogeographic impacts on traditional marine resources could explain socio-cultural changes (e.g., adoption of multi-family winter homes closer to alternative terrestrial resources) of Inuit between the late 17th and early 18th centuries on the Labrador coast [4,17,19–21]. However, other zooarchaeological studies, having documented few changes in the subsistence economy and a great capacity of adaptation of the Inuit through shifts in location, hunting, and technology strategies, rather underlines the implication of socio-economic and historical variables, such as more frequent European contacts on social organization, economic production, seasonal settlement patterns, and Inuit traditions [4,6,19,21]. These findings demonstrate that the effects of the LIA on populations have been rather heterogeneous or mixed, and that the relationship between human and environmental or climatic factors is not always obvious and causal in nature.

Despite the complexity and multiplicity of factors involved, palaeoclimatic and palaeoenvironmental reconstructions allow for the development of a framework at local and regional scales to evaluate how climate fluctuations and landscape changes may have influenced human populations in Labrador and assess how they adapted, while identifying the impacts they may have had, in turn, on adjacent ecosystems [14,18]. Multidisciplinary approaches that combine archaeological and palaeoenvironmental research help to evaluate these hypotheses by documenting how human societies and their immediate environment have changed over time [4,14]. While palaeoecological studies in the Nain Archipelago have addressed some of these gaps and contributed to the development of detailed reconstructions in terrestrial environments, they mostly overlook the dynamics and trajectories of lake ecosystems, and, therefore, additional information is needed to establish a more comprehensive palaeoenvironmental and palaeogeographic context.

1.2. Palaeogeographic Context

Since the deglaciation of its coastline around 9500–8500 cal. yr BP, the Labrador Peninsula has undergone significant environmental changes related to postglacial palaeogeographic evolution and Holocene climatic fluctuations. The patterns and timing of deglaciation, marine transgression and regression, and glacio-isostatic rebound remain poorly documented

on the Labrador coast. Clark and Fitzhugh [22] estimated that marine transgression following coastal deglaciation occurred up to a height of 71 m in the Nain area [22,23]. Given the low presence of shells in marine deposits, their proposed relative sea level curve for the Nain region is largely based on dating of charcoal recovered from Dorset and Maritime Archaic summer coastal archaeological sites under the assumption that the campsites were located close to the shoreline and the marine limit (1–2 m above the high water mark) [22]. A major limitation of charcoal dating is the "old wood" effect and the potential time lag between the cutting or death of the tree and its use [24]. In addition, the low resolution of available dates, few of which are derived directly from sediments at the marine boundary, restricts the accuracy of this curve. The compilation of radiocarbon data from the east coast of Canada by Vacchi et al. [23] allowed for the development of several relative sea level curves and estimates of the magnitude of glacio-isostatic adjustment over the past 16,000 years. Because the dates incorporated into their model for the central Labrador coast region (Okak to Hopedale) are primarily derived from archaeological sites presented by Clark and Fitzhugh [22] and the Canadian Archaeological Radiocarbon Database (CARD), they do not significantly improve the previously proposed curve and, furthermore, highlight the need for additional investigations to achieve more detailed reconstructions of Labrador coastline palaeogeography [23,25].

1.3. Palaeoclmatic Context

Palaeoecological studies that focused on the Labrador region revealed the spatial and temporal heterogeneity of Holocene climate fluctuations [2,18,26,27]. In particular, they reported considerable lags in the onset of important postglacial climatic periods, such as a later onset of the Holocene Thermal Maximum, as compared to neighbouring Arctic and subarctic regions and different response times between terrestrial (via dendroecology and pollen analyses) and aquatic (via diatoms, dinokysts, and Chironomidae) observations [2,10,11,27]. Moreover, several studies suggested that the magnitude of late Holocene climate fluctuations was less pronounced in the Quebec–Labrador Peninsula, resulting in limited directional changes within biological communities since the gradual Neoglacial cooling (ca. 3000 cal. yr BP) [27–32]. The few reconstructions based on lake and marine sediment cores from Labrador and Northern Quebec suggest that the climate and aquatic ecosystems of the region remained remarkably stable and resilient during the Late Holocene and since the last millennium, in contrast to what has been observed in other circumarctic regions [1,30–34].

The scarcity and short time span of the instrumental record (late 19th century), the considerable regional disparities, and the lack of spatial and temporal resolution of palaeoenvironmental reconstructions near settlement areas do not allow us to document, more precisely, the extent and specificity of environmental change in Labrador, particularly in lake ecosystems, in response to late Holocene climatic fluctuations (particularly Medieval Warm Period (MWP), LIA, and recent warming) and anthropogenic forcings. While palaeoenvironmental and geoarchaeological research has demonstrated that anthropogenic activities (e.g., wood harvesting) contributed to the transformation of the terrestrial landscapes of the Nain Archipelago concomitantly with late Holocene climatic variations, notably from the 17th to late 19th century [5–7,35–37], their effects on aquatic ecosystems have rarely been studied in the region.

As part of a larger multidisciplinary research initiative that focuses on different aspects, such as archaeology or palaeogeography, within the Nain Archipelago, the objective of this study was to reconstruct the postglacial palaeoenvironmental history and palaeoclimatic variability of Dog Island, on the subarctic coast of Labrador, and to document their effects on lake ecosystems within the context of human occupation. The development of such a framework can be used as a foundation for the development of deeper insights into human–environment relations in the northern Labrador coastal region. Lakes are often seen as sentinels of ecosystem change due to their sensitivity to climatic, ecological, and anthropogenic disturbances, which makes their sediments excellent natural archives that reliably record, with high resolution, the internal and external processes associated with

their watersheds [9]. To address these questions, we studied the physical, geochemical, and biological properties of lake sediment cores in close proximity to the Oakes Bay 1 (HeCg-08) archaeological site in parallel with dating methods [9].

2. Study Site

The geomorphology of the north-central coast of Labrador in the Nain area (Figure 1) consists of a plateau incised and eroded by large eastward-flowing rivers, open bays, and long glacial valleys perpendicular to the coast [38,39]. The region is part of the Nain geological province and underlain by the Precambrian Canadian Shield, which consists mainly of gneiss, granite, and anorthosite [38]. In addition to marine and coastal ecosystems, Labrador has many lakes, rivers, and wetlands, while permafrost is found discontinuously and sporadically across the landscape [39].

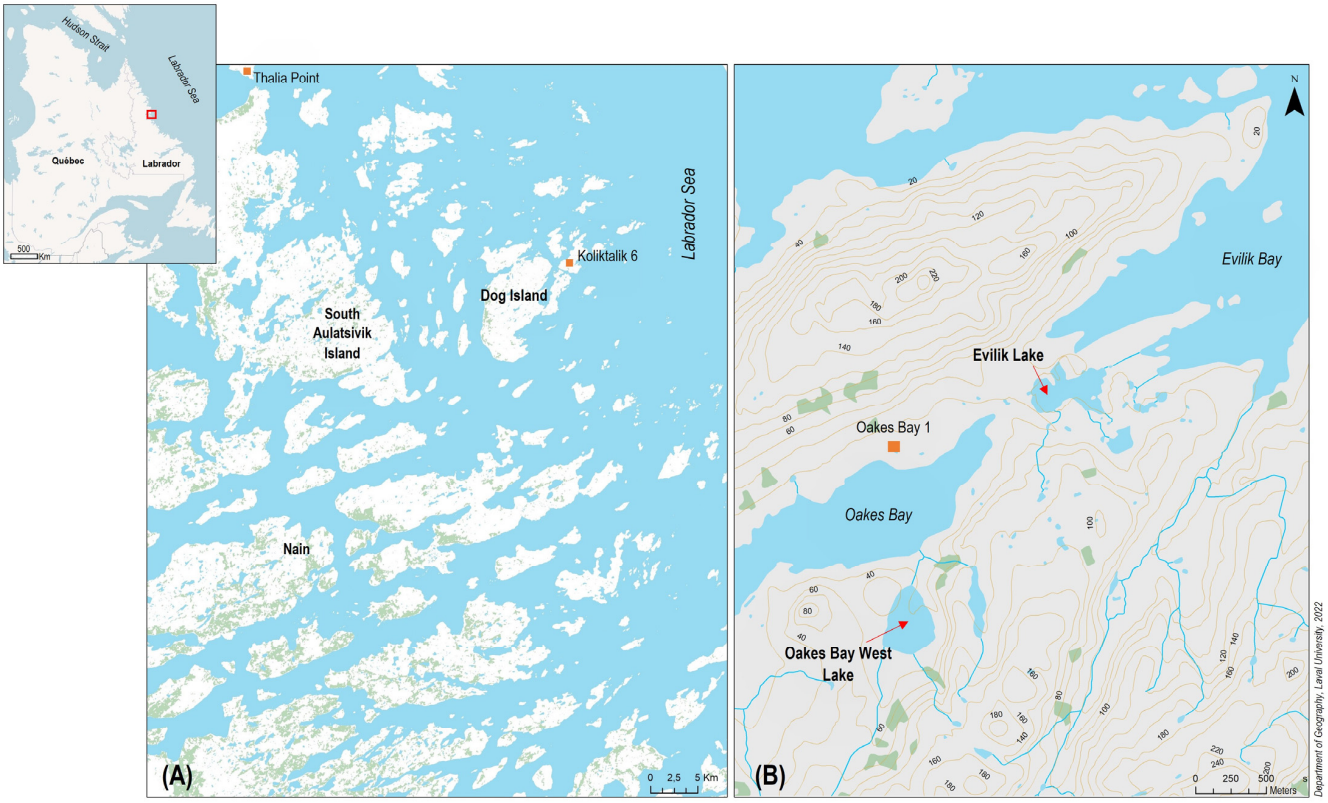

Figure 1. Location of the study site on the Labrador coast, Canada. (**A**) Nain and its Archipelago; (**B**) northern part of Dog Island showing sampled lakes, elevation (meters), and Oakes Bay 1 archaeological site.

The Nain Archipelago lies at the transition of the Arctic and subarctic climatic regions. The influence of the ocean–atmosphere nexus in the North Atlantic (e.g., North Atlantic Oscillation, Atlantic Multidecadal Oscillation, Arctic Oscillation) and of the Labrador Current on the coastal climate regime and the spatial and ecological dynamics of Nunatsiavut ecosystems has been documented [3,26,40,41]. The interplay of cold air masses from the Arctic, as well as warm, moist air masses from the Atlantic, results in long, cold winters and cool summers on the coast [27,42]. The average annual temperature is about −3 °C, and annual precipitations are distributed throughout the year, for a total of over 800 mm [42].

The terrestrial landscape of the Nain region, located in the coastal ecological zone, is characterized by tundra and forest tundra vegetation. Forest stands generally develop in protected valleys and near large bays with more favourable soils and climatic conditions, while well-drained portions of the land are covered by bare tundra [43,44]. Modern tree cover in sheltered areas is dominated by black spruce (*Picea mariana*), white spruce (*Picea*

glauca), and tamarack (*Larix laricina*), whereas on the coast, some trees are limited to the krummholz form. Current vegetation is dominated by shrubs (*Empetrum nigrum*, *Rubus chamaemorus*, *Ledum groenlandicum*, *Vaccinium* spp., *Kalmia angustifolia*), dwarf birch (*Betula glandulosa*), alders (*Alnus* spp.), and willows (*Salix* spp.) [6,27,29,35]. Graminoids, grasses (Cyperaceae), mosses, and lichens are also present [27].

Nain is the northernmost village in Labrador and the administrative capital of Nunatsiavut. It is bordered to the east by several offshore islands, which form the Nain Archipelago, and by the Labrador Sea (Figure 1). The two lakes sampled for this study are located on Dog Island (56°39′52.873″ N, 61°6′55.559″ W), located approximately 35 km northeast of Nain.

Oakes Bay West Lake (56°39′24.188″ N, 61°8′47.544″ W) lies approximately 300 m south of Oakes Bay, the main east–west-oriented bay of Dog Island, and approximately 500 m south of the Oakes Bay 1 archaeological site (HeCg-08) (Figure 1). This lake is located at an elevation of approximately 40 m above sea level (a.s.l.), and it is surrounded by hills, including two steep rock cliffs to the west and east and a few spruce patches to the south. At the northern end of Oakes Bay West Lake lies a peatland, composed mostly of *Sphagnum* and brown mosses. A previous core was taken at this site and was analysed for pollen content by Roy et al. [5], the results of which will be used for comparison with results obtained from diatom analysis in this study. Oakes Bay West Lake is oligotrophic, circumneutral, and has a maximum depth of 23.4 m (Table 1).

Table 1. Summary of physicochemical characteristics of Oakes Bay West and Evilik lakes (16 July 2019).

Lake	Oakes Bay West	Evilik
Coordinates	56°39′24.188″ N 61°8′47.544″ W	56°39′53.762″ N 61°7′05.19″ W
Altitude (m asl)	40	14
Maximum depth (m)	23.4	6.2
Area (km^2)	0.11	0.12
pH	6.83	7.13
Temperature surface (°C)	10.34	12.2
Temperature bottom (°C)	5.32	9.8
Conductivity (µS/cm)	53.4	71.12
* DO (mg/L)	12.83	11.35
* DOC (mg/L)	2.4	3
* DIC (mg/L)	1.5	1.9

* Note: DO, dissolved oxygen; DOC, dissolved organic carbon; DIC, dissolved inorganic carbon.

Evilik Lake (56°39′53.762″ N, 61°7′05.19″ W) is located in a more open landscape at an elevation of 12 m a.s.l. at the interface between Oakes Bay to the west and Evilik Bay to the east. It is shallower (~6.2 m), has a rockier and sandier bottom, and its waters are circumneutral and oligotrophic. Oakes Bay West and Evilik Lakes are located adjacent to known and studied archaeological sites, such as Oakes Bay 1 and Evilik 2 [4,5,7,19–21].

3. Materials and Methods

Two sediment cores from Oakes Bay West and Evilik lakes were retrieved in July 2019 using a UWITEC percussion corer equipped with 9 cm-diameter plastic tubes. Taken at the deepest part of the lake, the sediment sequence from Oakes Bay West (82.5 cm long) was recovered at a water depth of 23 m, while that from Evilik (94 cm long) was taken at a depth of 6 m. A physicochemical profile of the water column was also conducted on the same day with a multi-parameter probe, and surface water samples were collected and sent to the National Water Research Institute (Burlington, ON, Canada) to analyse current physicochemical properties of the lakes (Table 1). Polystyrene (floral) foam bricks were used to stabilize water–sediment interfaces of the cores prior to transport and storage in a cold room (4 °C) at Université Laval's Aquatic Paleoecology Laboratory (Québec City, QC, Canada).

Coring tubes were cut lengthwise, and sediments were split into two halves. One half of each core was sent to the Chrono-Environnement laboratory (UMR 6249 National Center for Scientific Research, University of Franche-Comté, France) for further analysis (geochemistry, dating of upper sediment layers and chironomids). In addition to new pollen analyses performed at the Geotop research center (Université du Québec à Montréal, Montréal, QC, Canada) on the two lake sediment cores, the results of all analyses will allow for future comparisons with our diatom data.

Prior to subsampling, half-cores were subjected to the Specim Labscanner hyperspectral scanner equipped with two cameras (VNIR: 400–1000 nm; SWIR: 1000–2500 nm) to obtain high-resolution images of sedimentary sequences. The half-cores were then subsampled at 0.5 cm intervals and stored in plastic Whirlpak® bags. One part of these samples was used for pollen analysis, while the other part was weighed and freeze-dried for 48–72 h. Subsequent analyses were performed on the dried samples.

3.1. Dating and Chronology

Given the lack of sufficient plant macrofossils found during subsampling, core chronologies were derived from radiocarbon (^{14}C) dating of bulk organic sediment samples via accelerator mass spectrometry (AMS). Six samples from Oakes Bay West and five from Evilik, taken at different depths and 0.5 cm-thick, were prepared and dated at the Centre for Northern Studies' Radiochronology Laboratory (Université Laval, Québec, QC, Canada) and at the Keck Carbon Cycle AMS Facility (University of California, Irvine, CA, USA).

Age-depth models were built with the rbacon package version 2.5–7 in R [45]. Based on Bayesian statistics, this model directly calibrates radiocarbon dates with the IntCal20 curve, estimates sediment accumulation rates (yr cm^{-1}), and generates the 95% (2σ) confidence interval age distribution as well as the mean and median ages of each sample [45–47].

3.2. Organic Matter and Water Content

Water content of the sediment was estimated by weighing the samples before and after being freeze-dried for a minimum of 48 h. Loss on ignition (LOI) was performed at 1 cm intervals on both cores following the method of Heiri et al. [48] to estimate the proportion of organic matter. Approximately 0.35 g of freeze-dried sediment was transferred to crucibles and dried at 105 °C for 24 h to remove any residual moisture. After weighing, they were placed in an oven at 550 °C for 5 h before being weighed again.

3.3. Grain Size Analysis

Grain size analyses were performed at the Geomorphology and Sedimentology Laboratory of Département de géographie (Université Laval) at 1 cm intervals on the LOI residues with an LA-960 Horiba Laser Particle Size Analyzer in order to detect changes in material source, transport mechanisms, and hydrologic regime over time [49]. Particle size distribution composing the samples and the statistical parameters (mean, median, sorting index) were determined with the GRADISTRAT v. 8.0 software [49] according to the arithmetic method of statistical moments.

3.4. Magnetic Susceptibility and Geochemical Analysis

Magnetic susceptibility of the sediments was measured with a Geotek MSCL (Multi-Sensor Core Logger) at a resolution of 0.5 cm on the half-cores to infer past minerogenic inputs from the watershed. Geochemical composition and relative element concentration of the sediments were obtained by X-ray microfluorescence (µ-XRF) measurements using an Avaatech Core Scanner at 500 µm intervals on the same half-cores. The relative concentrations of each detected element, originally expressed in peak area integrals, are presented as ratios (reported as log-ratios of intensities) to minimize possible interferences due to the heterogeneity of the sedimentary matrix [50–52]. Key elements displaying high signal-to-noise ratios and elemental ratios were selected for further analyses and to infer past changes in sediment inputs (Ti, K), primary productivity (Ca/Ti, Si/Ti), redox conditions (S, Fe/Ti, Mn/Ti, Mn/Fe), and marine influence (Br, Sr/Ti) [53].

Stratigraphic zones were identified by constrained hierarchical clustering with the constrained incremental sum of squares (CONISS) agglomerative method performed on geochemical data, previously standardized and transformed into a Euclidean distance matrix with functions available in the vegan and rioja packages in R [54,55]. The number of significant zones was determined with the broken-stick model [56].

3.5. Diatom Analyses

Identification and counting of diatom valves were performed at 0.5 cm intervals for the top two core centimetres to achieve finer temporal resolution of recent changes, and then at regular 2 cm intervals for the remainder. Additional samples were also analysed at interfaces of visible changes in sediment colour and texture. In total, 52 samples from each core were prepared and cleaned of organic matter for diatom analysis following the method of Scherer (1994) [57]. For each sample, approximately 0.06 g of freeze-dried sediment was treated with 30% hydrogen peroxide (H_2O_2) for 24 h to destroy organic matter. The samples were then heated in a water bath at 60 °C for 3 h before being left to decant for at least 24 h, then diluted and rinsed with distilled water until a neutral pH was obtained. Two dilutions consisting of the silica solution and distilled water were prepared for each sample, into which a known number of microspheres (initial concentration 6.19 × 106/mL; diameter ~8 µm) were added, according to the method of Battarbee and Kneen (1982) [58]. Thus, 0.5 mL of each solution was transferred to a coverslip and dried at room temperature before being permanently mounted on glass microscope slides with the synthetic resin Naphrax®.

Between 400 and 500 diatom valves were counted per sample and identified at the smallest possible taxonomic scale along random horizontal transects with a Zeiss Axio Imager 2 microscope (×1000 magnification under oil immersion). Other organisms encountered (silicoflagellates, cysts of chrysophyceae) as well as microspheres were also counted along the transects. The main taxonomic references consulted for nomenclature and identification were Krammer [59–61], Krammer and Lange-Bertalot [62–65], Campeau et al. [66], Fallu et al. [67], Witkowski et al. [68], Lange-Bertalot [69], Antoniades et al. [70], Zimmermann et al. [71], and Lange-Bertalot et al. [72]. Relative abundance of each identified taxon was calculated as the percent of the total number of valves counted by level, and diversity was estimated with Hill's N2 index. Results were summarized in a percentage diagram with the C2 software version 1.7.6 [73].

Significant biostratigraphic zones were identified using constrained hierarchical clustering analysis (CONISS) with a Bray–Curtis matrix as the dissimilarity measure and the broken-stick model [56].

3.6. Numerical Analyses

Multivariate statistical analyses were performed with R v.4.1.3 and RStudio software to detect major changes that occurred over time [74,75]. Only species whose relative abundance represented ≥1% in at least one level were included in the statistical analyses, and for statistical comparability, missing levels in the geochemical data (i.e., centimetres 82 and 83) were removed.

To better visualize and summarize the main patterns of variation and correlation among variables, an unconstrained ordination with principal component analysis (PCA) was conducted on Hellinger-transformed diatom relative abundance data and on the standardized physicochemical variables (elemental ratios included as supplementary proxies) using the vegan package (Figures S1 and S2) [76].

4. Results

4.1. Oakes Bay West Lake

4.1.1. General Stratigraphy

The Oakes Bay West core (82.5 cm long) consists entirely of lacustrine sediments (no marine or littoral sediment at the base). It presents three main zones: (1) a basal zone marked by a light grey unit of mineral sediments; (2) a more uniform dark-brown and

organic-mineral central section; and (3) an upper part characterized by the transition to a lighter grey-beige and slightly laminated mineral sediment matrix, with the return of dark-brown sediments at the 4 cm level.

4.1.2. Chronology

Results of ^{14}C dating of bulk sediment samples from Oakes Bay West and Evilik cores are summarized in Table 2.

Table 2. Radiocarbon and calibrated ages of sediments from Oakes Bay West Lake and Evilik Lake.

Lab Number	ID	Depth (cm)	Material	Conventional Radiocarbon Age (^{14}C Year BP)	Calibrated 2σ Age Interval (cal. Year BP)	Calibrated Median/ Mean Probability (cal. Year BP)
	Oakes Bay West Lake					
ULA-9764	OB13	13–13.5	Bulk sediment	1645 ± 15	1418–1568	1530/1520 *
ULA-9774	OB23	23–23.5	Bulk sediment	1680 ± 20	1531–1689	1570/1580
ULA-9775	OB39	39–39.5	Bulk sediment	2280 ± 15	2181–2345	2330/2300
ULA-9776	OB67	67–67.5	Bulk sediment	3730 ± 15	3987–4150	4080/4070
ULA-9777	OB76	76–76.5	Bulk sediment	5320 ± 20	6001–6192	6080/6090 *
ULA-8952	OB82	81.5–82	Bulk sediment	4320 ± 20	4840–4960	4860/4880
	Evilik Lake					
ULA-9778	EL12	12–12.5	Bulk sediment	745 ± 15	663–690	680/680
ULA-9779	EL25	25–25.5	Bulk sediment	1265 ± 15	1173–1275	1230/1230
ULA-9763	EL41	41–41.5	Bulk sediment	1920 ± 15	1747–1888	1840/1840
ULA-9762	EL69	69–69.5	Bulk sediment	2740 ± 15	2779–2865	2820/2820
ULA-8951	EL93	92.5–93	Bulk sediment	2060 ± 20	1942–2101	2020/2010 *

* Date considered erroneous and excluded from analyses; + median and mean calibrated date, rounded to the nearest decade.

Dates obtained from samples at 76 and 13 cm depth from Oakes Bay West were considered as possibly erroneous and were excluded from the age model. Being located at the border of what appears to be sudden sedimentary input events, these anomalous ages could be the result of old allochthonous carbon inputs from the watershed into the lake [77,78]. Potential influences on the accuracy of radiocarbon dates, such as the hard-water effect causing an overestimation of ages or incorporation of younger carbon through bioturbation or erosion (resulting in underestimated dates), should also be considered.

According to the age-depth model, the sedimentary sequence of Oakes Bay West covers a time interval of ca. 4900 cal. yr BP (Figure 2). Variations in sediment accumulation rates, as estimated by the model, followed the observed pattern of stratigraphic change, with slightly faster accumulation in the 80–68 cm and 10–4 cm intervals (40–55 yr cm^{-1}), and more stable and slower accumulation rates between 68–10 and 4–0 cm (55–75 yr cm^{-1}).

4.1.3. Lithology

LOI and water content analyses revealed significant changes following the two light-coloured zones at the base and the top of the core (Figure 3). Notably, these intervals (76–68 cm and 21–4 cm) were characterized by a rapid and abrupt transition to a mineral sedimentary matrix, low in organic matter (OM) and water content (WC). Initially low (OM: 6.7–9.9%; WC: 55–67%), organic matter and water content dropped drastically in sub-Zone 1b (76–68 cm) (OM: 2.8–1.7%; WC: 29–48%). This was accompanied by a significant increase in magnetic susceptibility, with the highest values recorded. Central Zone 2 (68–22 cm) was more homogenous, marked by a return to higher values of organic (6.4–15.5%) and water (60.4–80.2%) contents and low magnetic susceptibility. Peaking at 39–40 cm, organic matter and water content values progressively decreased throughout sub-Zone 2b (40–22 cm). The abrupt drop in the 21–4 cm interval (OM: 2.4–6.3%; WC: 37.9–62.7%) marked the beginning of Zone 3 (22–0 cm), while magnetic susceptibility displayed an inverse trend. Finally, a return to initial values was observed within the upper four centimetres (OM: 11.1–17.9%; WC: 69.9–85.9%).

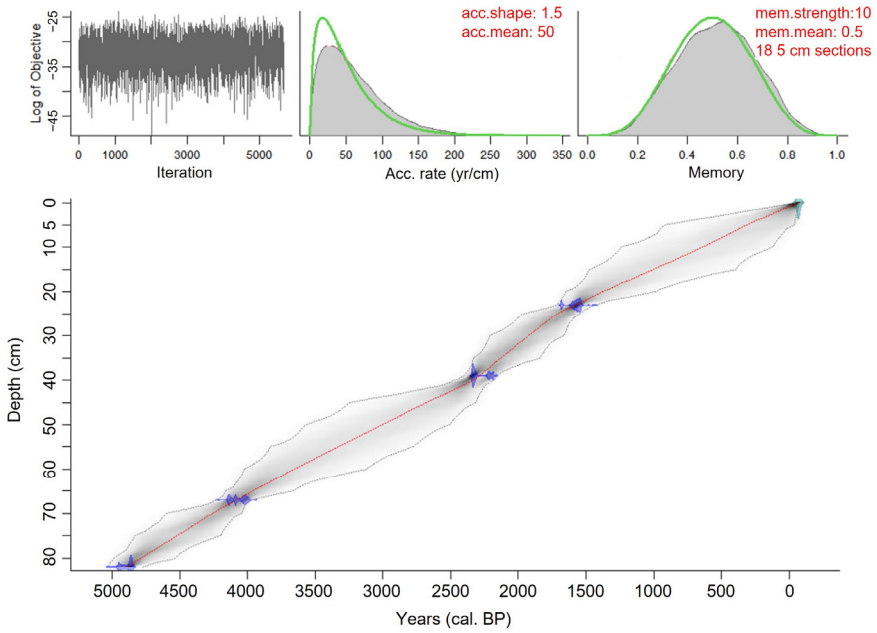

Figure 2. Bayesian age-depth model of Oakes Bay West Lake. The top panels represent, from left to right: MCMC iterations (model stability), prior (green lines) and posterior (gray) distributions for accumulation rate (middle panel), and model memory properties (right panel). The calibrated ages of the 4 dated samples (^{14}C) and their probability distribution are shown in blue. The grey area bounded by the dashed lines represents the age model with the 2σ (95%) confidence interval, and the red line indicates the weighted mean age corresponding to the most probable date.

4.1.4. Grain Size

The sediments generally exhibited a unimodal, sometimes bimodal, distribution and remained very poorly sorted throughout the core. The sediment matrix consisted mainly of silt, ranging from very fine to very coarse (2–63 μm), and sand (63 μm–2 mm) (Figure 3). Sediments of Zone 1, particularly of sub-Zone 1b (76–68 cm), were finer than in the rest of the core. They consisted predominantly of silt (silt: 74–53%; sand: 25–47%) and presented the only incursion of clay (<2 μm) in the core. Zone 2 showed a highly variable grain size pattern, where the proportion of sand was higher (silt: 32–56%; sand: 67–43%). In general, grain size increased in sub-Zone 2a, before dropping at the 40–39 cm level and rising again in sub-Zone 2b. A significant decrease in grain size was recorded between 21 and 20 cm, marking the beginning of Zone 3 (22–0 cm). This interval showed an extremely variable pattern, alternating between very coarse silt (31–63 μm) and fine sand (125–250 μm) before stabilizing within the last 10 cm, which was generally finer.

4.1.5. Geochemical Data

X-ray microfluorescence analysis provided the relative concentration of 20 elements (Na, Mg, Al, Si, P, S, Ar, K, Ca, Ti, Mn, Fe, Ni, Cu, Zn, Br, Rb, Sr, Zr, and Pb) in the sediment cores, 6 of which (Ti, K, Si, Ca, Fe, and Mn) were selected for their palaeoenvironmental significance in Oakes Bay West Lake.

The core showed rapid and major fluctuations in sediment geochemical composition and concentration, which were predominant in the detrital element profiles and closely followed the visible patterns in the stratigraphy (Figure 3). These were positively identified by clustering analyses (CONISS) and PCA (Figure 3 and Figure S1), which recognized six significant zones (three main, each divided into two sub-zones). Zone 1b (76–68 cm) was characterized by a rapid and major increase in detrital elements (Ti, K, and Si) and a decrease in primary productivity ratios (Si/Ti and Ca/Ti). Marked by a drastic decrease in detrital elements, Zone 2 (68–22 cm) was more stable. Values of Si/Ti and Ca/Ti ratios initially increased in Zone 2a (68–40 cm) but decreased progressively upwards in sub-Zone

2b. Comparatively less drastic than in sub-Zone 1b, sub-Zone 3a (22–10 cm) was again characterized by a rapid increase in detrital element (Ti, K) concentrations at the 21–18 cm level before gradually decreasing afterward. Conversely, Si/Ti and Ca/Ti values displayed a marked decrease in sub-Zone 3a but remained low for the rest of the core. The Mn/Fe ratio also decreased punctually in sub-Zone 3a, before rising again in sub-zone 3b (10–0 cm).

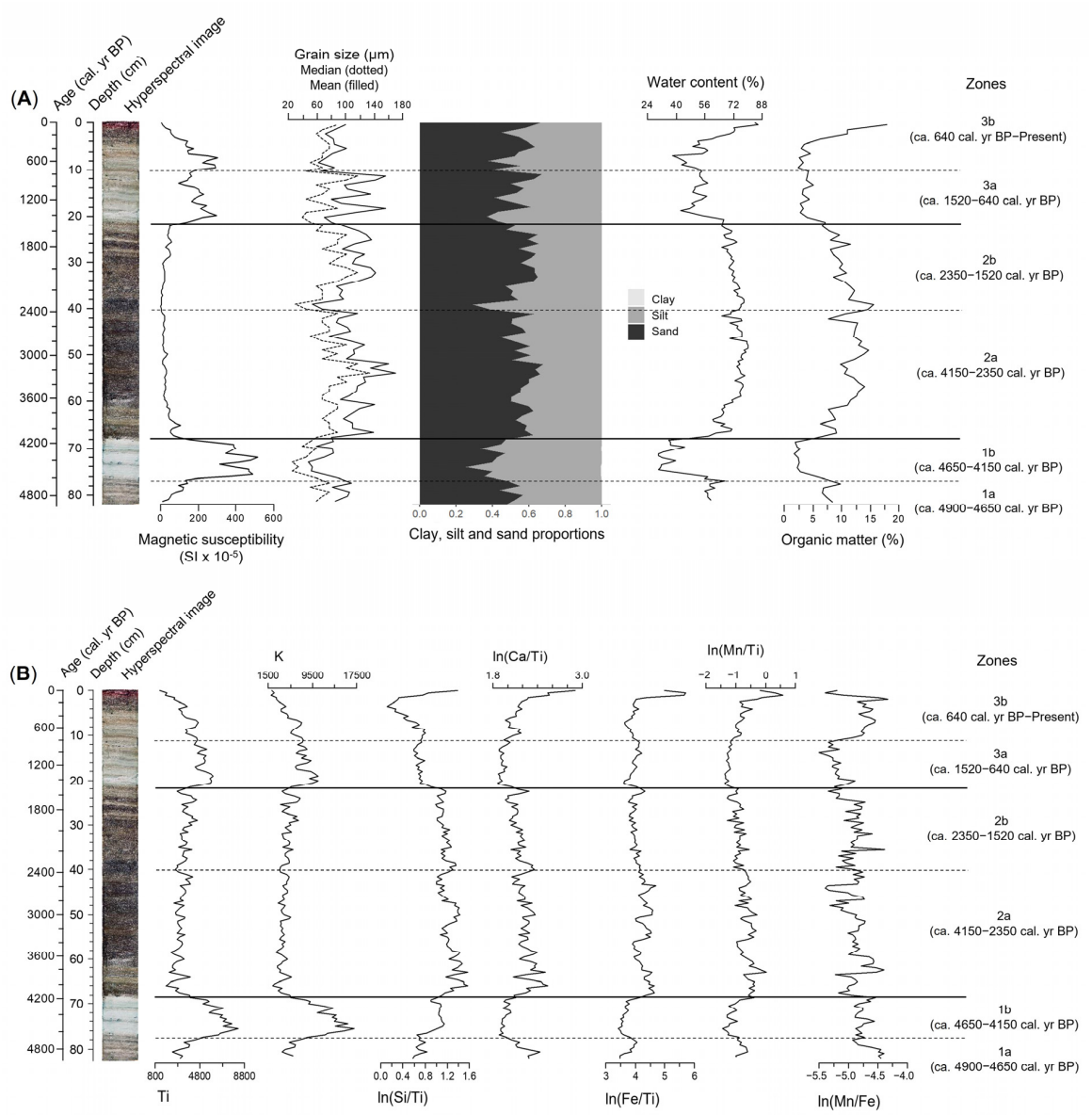

Figure 3. (**A**) Oakes Bay West Lake core litho-sedimentological profiles and significant stratigraphic zones (CONISS); (**B**) geochemical profiles (µ-XRF) of the Oakes Bay West Lake core and significant stratigraphic zones (CONISS). The two main events are identified by sub-Zones 1b and 3a.

4.1.6. Diatom Data

In total, 247 diatom species belonging to 61 genera were identified in the Oakes Bay West core, of which 57 represent a relative abundance of ≥1% in at least one level. The most abundant species (≥4% in at least one level) were presented in order of appearance in the core, and some species within the same genus were grouped together for graphical representation (Figure 4). Three significant biostratigraphic zones were identified with hierarchical clustering analysis (CONISS) and confirmed with PCA, which generally concorded with the main physicochemical zones previously described.

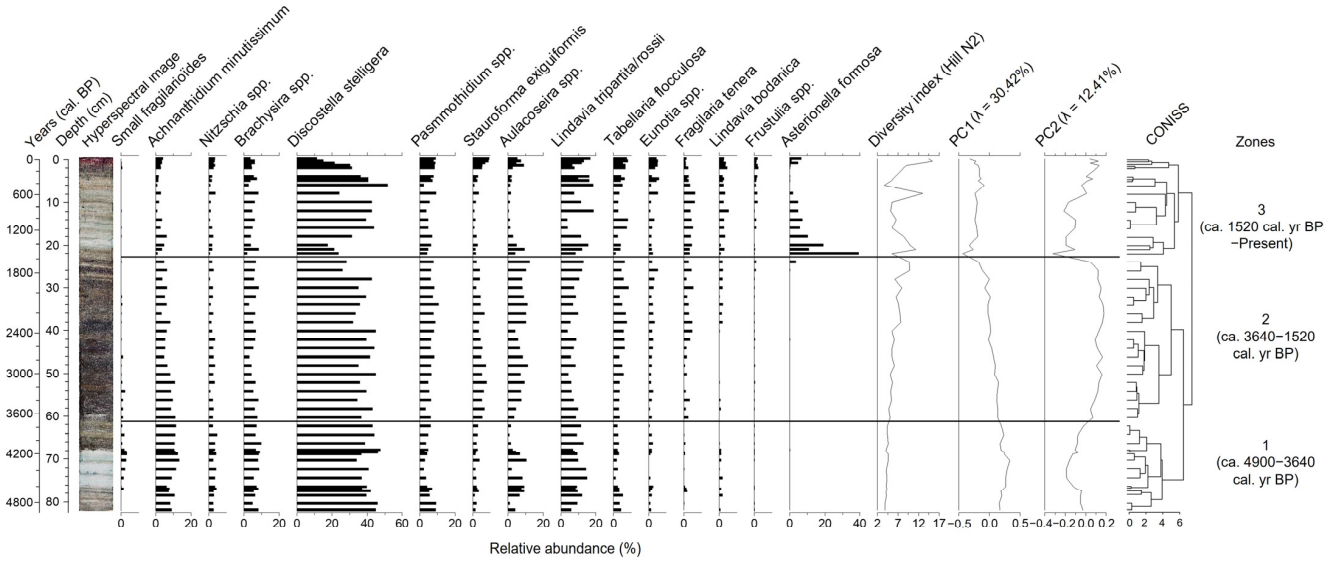

Figure 4. Relative abundance (%) of the most common diatoms (≥4% in at least one level), diversity index, sample coordinates along the two main PCA axes, and biostratigraphic zones (CONISS) of the Oakes Bay West Lake core.

Zone 1 (82.5–62 cm) was dominated by the small centric planktonic species *Discostella stelligera*, representing between 34.2 and 47.9% of the assemblage, as well as *Lindavia tripartita-rossii* complex (6.1–15.3%) and *Brachysira* spp. (5.3–10.1%). The alkaliphilic species *Achnanthidium minutissimum* (6.3–13.3%) and small fragilarioides (0–3.8%) reached their maximum abundances in this zone, while the highly silicified tychoplanktonic species of the genus *Aulacoseira* (1–10.7%) were particularly important in the inorganic pale sediment interval (77–68 cm) and decreased drastically thereafter. Diversity showed the lowest values of the entire core and increased very slightly in Zone 2.

The beginning of Zone 2 (60–42 cm) was marked by the dominance of *Discostella stelligera* (35.4–45.1%) but also by an increase in *Aulacoseira* spp. (3.6–11.5%), *Psammothidium* spp. (3.4–8.3%), *Stauroforma exiguiformis* (4.6–8.2%), and *Tabellaria flocculosa* (3.1–5.7%). *Brachysira* spp. (3.2–8.6%) as well as *Lindavia tripartita-rossii* (4.4–10%) were still present but decreased slightly up to 40 cm. The abundance of the alkaliphilic taxa *Achnanthidium minutissimum* (3.4–11.2%), *Nitzschia* spp. (0.8–3.7%), and small fragilarioides (0–2.7%) gradually decreased throughout Zone 2, particularly from 46 cm. At 40 cm, a punctual decrease in *Aulacoseira* spp. (4.6%), *Lindavia tripartita-rossii* complex (3.9%), and *Stauroforma exiguiformis* (3.5%) marked the beginning of a reorganization for the remainder of Zone 2 (40–24 cm). The latter interval was characterized by an increase in the acidophilic *Eunotia* spp. (0.8–5.3%) taxa, *Fragilaria tenera* (0.2–5.4%), and *Lindavia bodanica* (0–2.4%), as well as a further increase in *Aulacoseira* spp. (8.2–12.5%), *Tabellaria flocculosa* (4.8–8.6%), *Psammothidium* spp. (6.2–10.7%), and *Lindavia tripartita-rossii* (5.7–13%). In contrast, *Stauroforma exiguiformis* (2.2–4.7%) and *Discostella stelligera* (26.4–43%) gradually decreased towards the end of Zone 2.

The beginning of Zone 3 (22–0 cm) was marked by a very large and punctual abundance of the species *Asterionella formosa*, which decreased from 39.5% to 5.1% in the 22–10 cm interval. Between 22 and 4 cm, there was a drastic decrease in *Achnanthidium minutissimum* (3.8–1%), *Stauroforma exiguiformis* (3.6–1%), and *Aulacoseira* spp. (2.4–0.8%). After a brief episode of lower abundance between 26 and 20 cm, *Discostella stelligera* rose (17.8–31.5%) again from 18 cm onwards, accompanied by *Brachysira* spp. (2.9–8.6%), *Psammothidium* spp. (4–9.5%), *Lindavia tripartita-rossii* complex (4–19%), *Lindavia bodanica* (2–5.5%), and *Fragilaria tenera* (2–6.5%). Finally, a rearrangement of species occurred within the last four centimetres with a decrease in *Fragilaria tenera* (2.6–1.1%) and *Discostella stelligera* (31.7–11.6%) and an increase in *Frustulia* spp. (0.4–2%), *Lindavia bodanica* (2.9–4.8%), *Eunotia* spp. (3.8–6%), *Tabellaria flocculosa* (5.6–8.4%), *Aulacoseira* spp. (3.0–9.2%), *Stauroforma*

exiguiformis (5.3–9.6%), and *Asterionella formosa* (0.4–6.9%). The beginning of Zone 3 was characterized by a higher diversity index between 22 and 18 cm, which decreased between 16 and 5 cm but rose again in the last 4 cm of the core.

4.2. Evilik Lake

4.2.1. General Stratigraphy

The Evilik core (94 cm long) consists of marine sediments overlain by lacustrine sediments. The base of the core comprises an olive-grey sandy matrix with pebbles and gravels. The central section is characterized by a finer matrix and shows a gradual transition to increasingly darker, finely laminated black sediments that alternate with thin pale sandy layers. Finally, the upper part consists of more uniform orange-brown organic-rich lacustrine sediments.

4.2.2. Chronology

Exhibiting an age inversion (Table 2), the basal date (92.5 cm) was excluded based on the very poor organic matter content of the bulk sediment sample and its apparently too-young age when compared with emersion curves proposed by the few studies of glacio-isostatic rebound in the region [22,23]. Because the lower levels are the result of extrapolation by the Bayesian model, and given the uncertainties associated with the dating of bulk organic sediments and possible influence of marine waters, we, therefore, can only suggest minimum dates for lake basin isolation.

According to the age-depth model, the sedimentary sequence of Evilik Lake covers an interval of ca. 3350 cal. yr BP (Figure 5). The estimated accumulation rate is initially faster between 94 and 72 cm (20 yr cm^{-1}), possibly reflecting high sediment availability, and gradually decreases between 70 and 62 cm (20–35 yr cm^{-1}) before holding steady until the 20 cm level (35–40 yr cm^{-1}). The upper levels of the core (18–0 cm) are characterized by a gradual slowing of the accumulation rate (40–65 yr cm^{-1}).

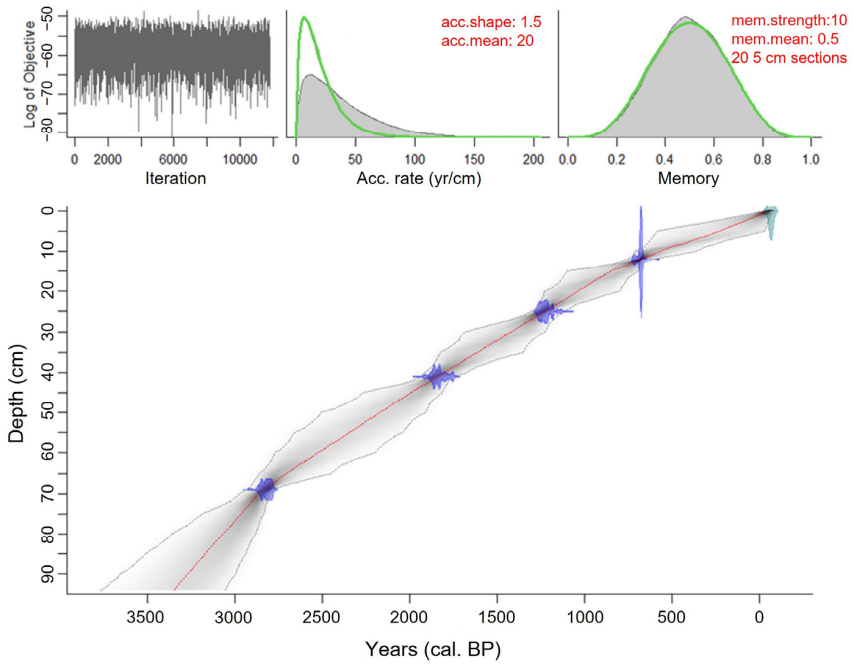

Figure 5. Bayesian age-depth model of Lake Evilik. Top panels represent MCMC iterations representing model stability, prior (green lines) and posterior (grey) distributions for accumulation rate (middle panel) and model memory properties (right panel). The calibrated ages of the 4 dated samples (^{14}C) and their probability distribution are shown in blue. The grey area bounded by the dashed lines represents the age model with the 2σ (95%) confidence interval, and the red line indicates the weighted mean age (the most probable date).

4.2.3. Lithology

Variations recorded in organic matter and water content, as well as magnetic susceptibility, are reflected in the three main zones observed in the stratigraphy (Figure 6). The basal part forming sub-Zone 1a (94–72 cm) was characterized by a very low proportion of OM (1.4–4.8%) and WC (19.2–42.4%), corresponding to the sandy matrix. Magnetic susceptibility values were at their highest, showing a sawtooth pattern with significant peaks. In sub-Zone 1b (72–64 cm), water and organic matter contents increased steadily (OM: 5.6–12.8%; WC: 50.5–71.4%), before dropping rapidly at the beginning of Zone 2 between 64 and 57 cm (OM: 8.6–6.5%; WC: 70.9–63.1%). Gradually increasing in a stepwise pattern, the two variables increased at the 56 cm level, remained relatively stable until 50 cm (OM: 10.2–13.8%; 72.1–79.1%), and then increased again abruptly at the 49 cm level. Organic matter and water contents increased progressively in the remainder of the core (OM: 14.3–26.6%; Water: 79.6–92.4%), with an isolated decrease at 45 cm (OM: 14.67%; Water: 64.4%) and a significant point drop in organic matter at 39 cm (OM: 9.5%) at the beginning of Zone 3 (44–0 cm). Magnetic susceptibility remained very low, with two higher peaks registered at 57.5 and 52 cm.

4.2.4. Grain Size

The grain size distribution showed a unimodal distribution, with extremely to very poorly sorted sediments throughout the core. The sediment matrix consisted of a larger proportion of sand and a varying proportion of silt (Figure 6). Zone 1 (94–64 cm) consisted of a dark olive-grey sandy matrix with pebbles (1–1.5 cm wide) and several gravels (>3 mm), particularly in Zone 1a. A gradual decrease in the sand proportion (99.5–62%) was noted in Zone 1. The average grain size also decreased from medium sand (250–500 µm) to very fine sand (63–125 µm), although peaks of high values were present at 73 and 67 cm. In Zone 2 (64–44 cm), the proportion of sand slightly increased (70.4–82.9%), with a higher proportion of very coarse sand (1–2 mm) between 56 and 44 cm. The mean and median grain sizes, corresponding to fine (125–250 µm) and medium (250–500 µm) sand, revealed episodes marked by the presence of coarser material. Indeed, the grain size peaked at 62, 56, and 51 cm, where gravels and pebbles were also found. Marked by a punctual drop in grain size at 40 cm, Zone 3 (44–0 cm) was characterized by a varying proportion of sand (64.1–84.3%) and a more stable mean and median size, which decreased in the last five centimetres from fine to very fine sand.

4.2.5. Geochemical Data

Among all elements measured, nine were selected for their palaeoenvironmental interests in Evilik Lake (Ti, K, Si, Ca, Fe, Mn, S, Sr, Br). The zones identified by clustering analyses (CONISS) and PCA (Figures 6 and S2) closely followed the observed changes in diatom assemblages, and geochemical profiles showed a clear evolution with three main stages: (1) a basal glaciomarine mineral zone, dominated by detrital and carbonate elements (94–64 cm); (2) a transitional middle section, characterized by redox-sensitive elements (64–44 cm); and (3) an upper lacustrine interval of organic sediments (44–0 cm) (Figures 6 and S2).

The basal Zone 1 (94–64 cm) was separated into two sub-zones. Sub-Zone 1a (94–72 cm) was rich in detrital elements (Ti, K) and marked by the significant presence of marine sediment constituents (Ca and Sr, which are fixed by calcifying organisms; Br, associated with organic matter of marine origin) [53]. Sub-Zone 1b (72–64 cm) was distinguished by an increase in Si/Ti ratio and a decrease in Sr, Ca, and Br values, while detrital elements (K, Ti) increased slightly and maintained high values. Zone 2 (64–44 cm) was characterized mainly by an increase in S and Fe/Ti values. The former peaked between 58 and 44 cm, while the latter increased gradually throughout Zone 2. These changes were accompanied by a progressive decrease in Mn/Fe and Mn/Ti values. Detrital elements remained high in the early part of Zone 2, before decreasing from 52 cm onwards, while Br values show significant peaks at 62 and 60 centimetres. Meanwhile, silica and biogenic carbonates (Si/Ti, Ca/Ti) increased very slightly throughout Zone 2. Sub-Zone 3a (44–32 cm) marked the

transition to the more stable conditions of sub-Zone 3b. This interval was characterized by a rapid decrease in S and a return to higher Mn/Fe and Mn/Ti values. Detrital elements, meanwhile, reached their minimum baseline values in sub-Zone 3a while Si/Ti and Ca/Ti ratios increased more significantly. The upper Zone 3b (32–0 cm), marked by a return to low Br and Fe/Ti values, was characterized by greater stability. Detrital elements were low, while Si/Ti and Ca/Ti ratios remained high.

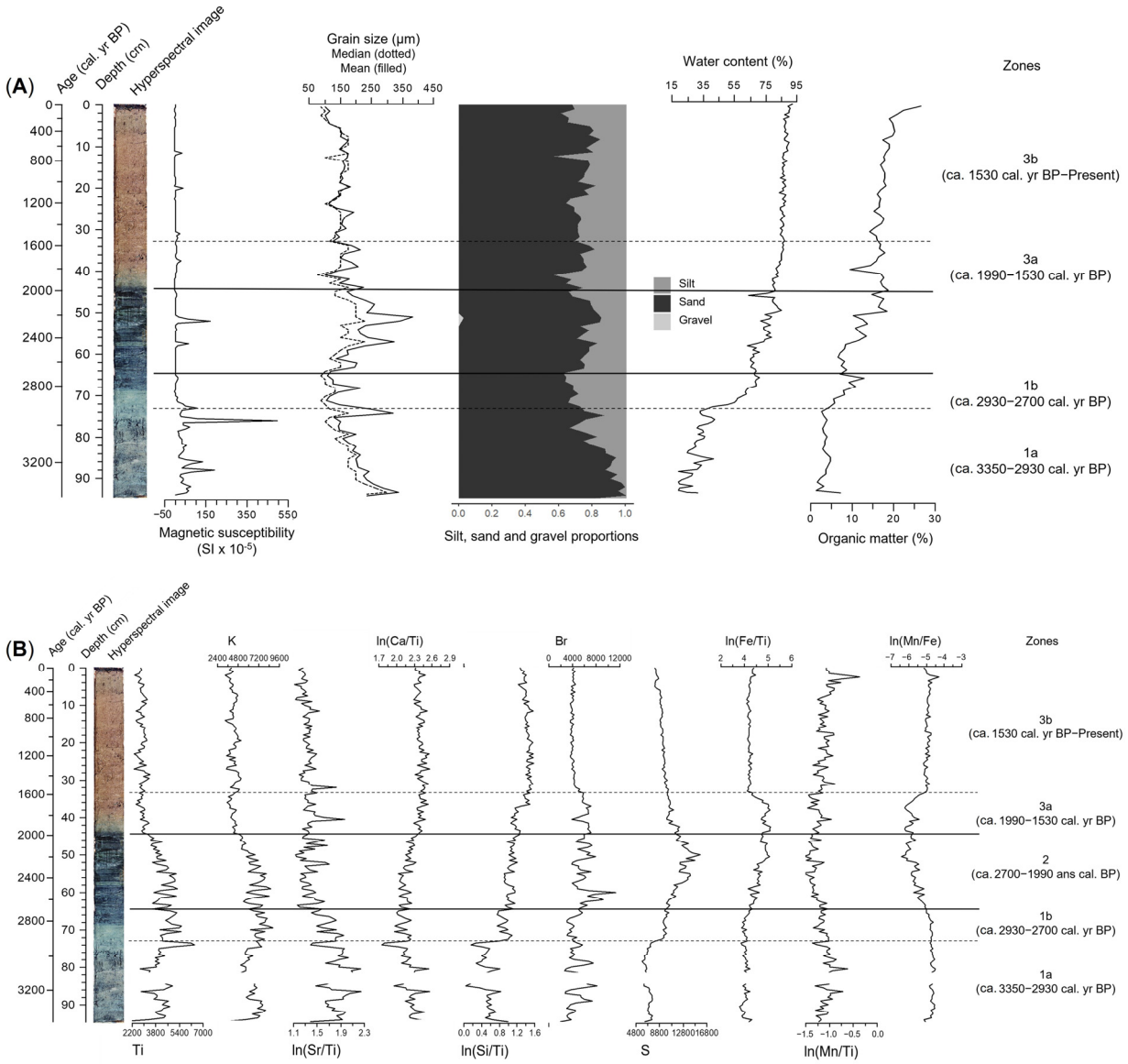

Figure 6. (**A**) Litho-sedimentological profiles of the Evilik Lake core and significant stratigraphic zones (CONISS); (**B**) geochemical profiles (µ-XRF) of the Evilik Lake core and stratigraphic zones (CONISS). The three main zones correspond, respectively, to the glacio-marine, brackish, and lacustrine phases.

4.2.6. Diatom Data

In total, 322 diatom species belonging to 95 genera were identified, reflecting a highly diverse coastal diatom flora. Of these, 115 were present with an abundance ≥1% in at least one level. The most abundant species (≥5% in at least one level) were classified into ecological groups according to their salinity tolerance based on the simplified halobian system presented in Campeau et al. [66]: polyhalobian (35–20‰), mesohalobian (30–0.2‰), oligohalobian-halophilous (affinity for lightly saline water), and oligohalobian-indifferent

(freshwater but tolerant of brackish water) [66]. Clustering analyses and PCA allowed us to identify three significant biostratigraphic zones, which were in agreement with the three main zones defined by the physicochemical variables (Figure 7).

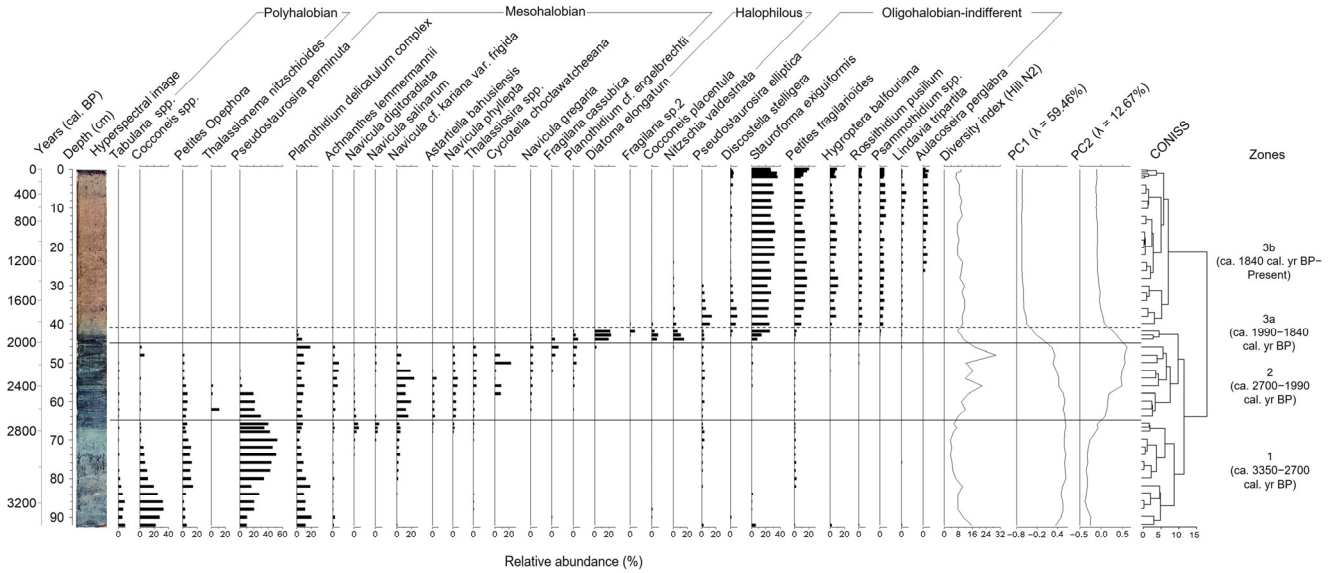

Figure 7. Relative abundance (%) of the most common diatoms (≥5% in at least one level), diversity index, sample coordinates along the two main PCA axes, and biostratigraphic zones (CONISS) of Evilik Lake.

Zone 1 was accumulated between 94 and 64 cm depth; its onset (94–82 cm) showed very low concentration and high fragmentation of diatom frustules. It was dominated by the polyhalobian species *Cocconeis* spp. (*scutellum*, *costata*, *stauroneiformis*, *peltoides*, aff. *neothumensis*; 20.3–34%), *Pseudostaurosira perminuta* (9.9–27.2%), *Planothidium delicatulum* complex (10.1–20.7%), *Tabularia* spp. (cf. *ktenoides*, *fasciculata*, *investiens,* and *waernii*; 3.8–9.6%), and, to a lesser extent, *Paralia sulcata* (2.5–5.1%). From 80 cm, the assemblages were marked by an increase in and dominance of *Pseudostaurosira perminuta* (34.1–52.7%), accompanied by an increase in the small claviform species of the genus *Opephora* (3.9–14.8%) as well as *Paralia sulcata* (2.9–5.8%) and *Navicula* cf. *kariana* var. *frigida* (1.8–5.5%). At the same time, there was a significant decrease in *Cocconeis* spp. (12.4–2.4%) taxa, the disappearance of *Tabularia* spp., and a slight progressive decrease in *Planothidium delicatulum* complex (3.2–12.8%). Toward the end of Zone 1, from 68 to 64 cm, there was a punctual increase in some euryhaline mesohalobian diatoms, including *Navicula digitoradiata* (3.9–7.2%) and *Navicula salinarum* (3.3–5.6%), accompanied by *Amphora beaufortiana*, *Caloneis crassa,* and *Pinnularia quadratarea*.

The diversity index, which was relatively low in Zone 1, increased in Zone 2 (64–44 cm) and peaked between 56 and 46 cm. The diatom assemblages in Zone 2 were characterized by an increase in the mesohalobian species *Navicula* cf. *kariana* var. *frigida* (12–24.6%), *Planothidium delicatulum* complex (6–19.2%), *Achnanthes lemmermannii* (1.8–9.1%), *Astartiella bahusiensis* (2.6–7%), *Navicula phyllepta* (2.6–8.4%), *Navicula gregaria* (0.8–4.6%), and *Thalassiosira* spp. (0.8–4.4%). The decrease in and disappearance, particularly after 56 cm, of the polyhalobian species of Zone 1 *Pseudostaurosira perminuta* (29.5–0%), small *Opephora* (7.3–0%), and *Paralia sulcata* (3.7–0.4%) was also noted. From 52 cm, *Navicula* cf. *kariana* var. *frigida*, *Navicula phyllepta,* and *Astartiella bahusiensis* suddenly decreased in favour of the new species *Opephora olsenii* (1–5.2%), *Planothidium* cf. *engelbrechtii* (1.6–5.2%), and *Fragilaria cassubica* (0–9.8%). The marine planktonic species *Thalassionema nitzschoides* made a spontaneous appearance at the 62 cm level (11.2%) and with less importance at 56 cm, while the mesohalobian planktonic *Cyclotella choctawatcheeana* was found with peak abundance at depths 58–56 (8.9–9.4%) and 50–48 cm (23.3–7.5%).

Zone 3a (44–40 cm) briefly marked the return of low diversity values and the disappearance of mesohalobian species. After a sudden and brief presence of some epiphytic halophilous and oligohalobian-indifferent species in sub-Zone 3a, namely *Cocconeis placentula* (3.9–9.2%), *Diatoma moniliformis/elongatum* (19.6–23.5%), and *Nitzschia valdestriata* (6.3–15.5%), sub-Zone 3b (40–0 cm) was characterized by the establishment of a diatom flora composed only of freshwater taxa typical of lakes in northern regions. The assemblages were dominated by the benthic species *Stauroforma exiguiformis* (22.4–36.5%), small fragilarioides (9.1–20.8%), *Hygroptera balfouriana* (2.6–11.2%), *Rossithidium pusillum* (2.4–5.5%), and *Psammothidium* spp. (2.5–8.5%). The beginning of sub-Zone 3b, from 40 to 30 cm depth, was marked by the isolated increase in *Pseudostaurosira elliptica* (14.3–3%) and *Discostella stelligera* (10–3.4%), while from 26 to 0 cm, the highly silicified tychoplanktonic species *Aulacoseira perglabra* (3.5–8.6%) appeared.

5. Discussion

5.1. Palaeoenvironmental and Palaeoclimatic Reconstruction of Oakes Bay West Lake

The Oakes Bay West Lake core exhibits a sequence divided into three main phases, with two contrasting events occurring between ca. 4650 and 4150 cal. yr BP and ca. 1520 and 640 yr cal BP (Figure 3, Zones 1b and 3a). Concordance of changes observed in sedimentological, geochemical, and magnetic property profiles allowed us to identify and characterize these sedimentary intervals that likely reflect episodes of greater erosion and terrigenous inputs. Otherwise, the observed changes in diatom assemblage composition coincide with transitions noted in regional terrestrial vegetation and are, overall, consistent with major episodes of climatic variation documented in North America and the North Atlantic Basin. Our evidence suggests a strong link between sedimentological processes occurring in the watershed, which may be associated with changes in vegetation cover and/or the hydrological regime (precipitation and runoff), major geophysical processes (landslides, earthquakes, etc.), and the observed changes in diatom assemblage composition and physicochemical properties in lake sediments.

Largely dominated by centric planktonic diatoms, particularly the species *Discostella stelligera*, the assemblages of Oakes Bay West are characteristic of deep oligotrophic and circumneutral to slightly acidic high-latitude lakes. The diatom flora surveyed has been found in various circumpolar regions across the northern treeline, including the Northwest Territories [79,80], northern Québec and Labrador [32,33,67], the Canadian Arctic [70], and southwest Greenland [81].

5.1.1. End of Holocene Thermal Maximum (ca. 4900–3640 cal. yr BP)

The large increase in detrital elements and magnetic susceptibility from ca. 4650 to 4150 cal. yr BP (Figure 3) suggests a short-lived sedimentation event, possibly generated by an initial destabilization in the watershed that would have resulted in the remobilization and transfer of terrestrial inorganic mineral material to the lake. Large sediment inputs, possibly caused by increased meltwater runoff in the context of warmer air temperatures and/or higher precipitations or a landslide, could have resulted in a large amount of suspended fine particles and reduced light in the water column. These conditions, and/or other modifications in stratification patterns (duration and mixing depth) related to seasonality changes, may have, in turn, favoured the punctual abundance of the planktonic species *Lindavia rossii* and *Aulacoseira tenella* at the expense of benthic species between ca. 4650 and 4150 cal. yr BP (Figure 4) [82,83].

The combined presence of some circumneutral-acidophilic (*Stauroforma exiguiformis*, *Psammothidium* spp., *Brachysira* spp.) and alkaliphilic species (*Achnanthidium minutissimum*, small fragilarioides, *Nitzschia* spp.), which subsequently decline or disappear, suggests slightly more alkaline initial conditions between ca. 4900 and 3640 cal. yr BP [83]. Small fragilarioid species are characteristic of northern oligotrophic lakes and recognized as "opportunists" adapted to highly variable conditions and short growing seasons given their rapid reproduction and growth rate [84]. They are abundant in assemblages of the

initial and alkaline phases of lakes, which are associated with base cation inputs from undeveloped and unweathered rocky soils, typical of recently deglaciated areas with sparse vegetation [79,85,86]. Leaching of glaciomarine deposits by meltwaters and disturbances in the watershed resulting in large sediment inputs into the lake could explain their slight increase during this time interval.

According to the age model, the basal part of the core was deposited between ca. 4900 and 3640 cal. yr BP. This interval is generally recognized as the end of the warm Holocene Thermal Maximum (HTM or "Hypsithermal"), which occurred later (after 7000 cal. yr BP) in Eastern Canada and southern Greenland than in Central and Northwestern Canada [27]. In Labrador, pollen assemblages suggest expansion and densification of vegetation cover around 4500 cal. yr BP [28,29]. On Dog Island, shrub tundra vegetation dominated by alder and birch prevailed between 5700 and 4800 cal. yr BP, while the increase in spruce pollen, likely favoured by warmer temperatures, marked the transition to a forest tundra between ca. 4800 and 3000 cal. yr BP [5]. These results agree with reconstructions from Baffin Bay in the Canadian Arctic [87] and southwest Greenland [88–92] that document warming of surface water temperatures, reduced sea ice cover, and increased meltwater runoff until about 3600–3200 cal. yr BP.

5.1.2. Neoglacial Period (ca. 3640–1520 cal. yr BP)

Between ca. 3640 and 1520 cal. yr BP, changes in the composition of diatom assemblages suggest a slight and progressive acidification of the lake and possibly windier conditions, as indicated by diatom composition. The timing and nature of the biostratigraphic changes closely match the onset of gradual neoglacial cooling and associated environmental changes. Although variable in time and space, this trend has been reported in the Quebec–Labrador region after 3500–3000 cal. yr BP [28,29,93,94] and proposed at several locations in the Canadian Arctic and southwest Greenland beginning around 3700–3000 cal. yr BP [90,91,95]. At surroundings of Nain village, *Picea* pollen percentages had significantly dropped about 2800 cal. yr BP, indicating a cooler climate [37]. On Dog Island, dry and cold conditions would have resulted in the opening of the forest canopy and a decline in spruce between ca. 3000 and 1140 cal. yr BP [5].

Like in our study, increased relative abundance of the larger and highly silicified (tycho)planktonic *Aulacoseira* complex, sometimes accompanied by periphytic *Stauroforma exiguiformis* and *Psammothidium* (*marginulata*, *altaica*), has also been observed in circumneutral to slightly acidic lakes in the Canadian Arctic, Northwest Territories, Yukon, and Greenland, where their dominance has been associated with periods of high winds and more vigorous mixing of the water column [79,96]. In this context, their greater presence during this interval (ca. 3640–1520 cal. yr BP) in the Oakes Bay area (Dog Island; Figure 4) may indicate windier conditions, when the opening of the landscape during the Neoglacial would have allowed winds to create the turbulence they require to maintain their position in the photic zone of the water column [83,97]. This is also suggested by Rühland and Smol (2005) in a study conducted in a subarctic lake in the Northwest Territories, who associate the increase in *Aulacoseira* species and concomitant decrease in dissolved inorganic carbon (DIC) around ca. 3470 cal. yr BP with more intense wind conditions following the retreat of the tree line and the development of a slightly more acidic environment in a cooling climate [80].

The close relationship between changes in alkalinity and the biophysical conditions of the watershed (e.g., plant succession and soil development) has been demonstrated in various arctic and subarctic lakes [79,85,86]. In Northern Quebec lakes, the increase in diatom-based dissolved organic carbon (DOC), water colour, and consequent gradual decrease in alkalinity, particularly after 3000 cal. yr BP, coincided with the arrival and prior expansion of spruce (*Picea mariana*) in the watershed [31,86]. Under this premise, the establishment of spruce on low-buffering granitic bedrock in the studied region between 4800 and 3000 cal. yr BP, the gradual paludification of the watershed, and the decrease in inorganic sedimentation could have, in the long term, contributed to the export of DOC,

the acidification of the lake, and the development of an acidophilic diatom flora (e.g., *Aulacoseira* spp., *Psammothidium marginulatum*, *Stauroforma exiguiformis*, *Tabellaria flocculosa*, *Eunotia* spp.), particularly after ca. 2400 cal. yr BP [5,83,98].

Another explanation raised for natural lake acidification refers to climate and associated variations in ice phenology and DIC dynamics, which may be a driving factor in biological communities in high-latitude lakes characterized by restricted vegetation and soil development [96,99]. The relationship between climate and pH, through ice cover and internal lake processes responsible for DIC speciation, has been documented in weakly buffered oligotrophic lakes in the Canadian Arctic during the late-Holocene climatic deterioration, particularly after 3000–2500 cal. yr BP [96,98,99]. In this context, increased duration and extent of ice cover, preventing CO_2 escape to the atmosphere and limiting light and primary productivity, could result in decreasing lake pH [96]. The succession of assemblages throughout this zone, marked by the emergence of acidophilic diatoms to the detriment of alkaliphilic taxa, suggests slightly more acidic conditions that are also consistent with the impacts, albeit subtle, of a gradual cooling of moderate magnitude [96]. Furthermore, the decrease in detrital elements (Figure 3) also suggests limited sedimentary inputs, possibly through a decline in meltwater runoff.

Abundance of *Discostella stelligera* in modern lake sediments has often been associated with changes consistent with warmer temperatures, such as decreasing ice cover extent and duration, enhanced thermal stratification, or shallow water mixing depths that, in turn, influence light availability and nutrient distribution [1,83,100]. The decrease in *Discostella stelligera*, particularly after ca. 2400 cal. yr BP, therefore, likely indicates changes in the thermal structure of the lake, including a period marked by greater vertical mixing of the water column or reduced stratification (duration and strength) favoured by short growing seasons and/or cooler summer temperatures, as implied by the increase in taxa belonging to the genus *Aulacoseira* [80].

5.1.3. Roman and Medieval Warm Periods to Present Conditions (ca. 1520 cal. yr BP–Present)

Biostratigraphic assemblages and physicochemical profiles reveal rather variable conditions since ca. 1520 cal. yr BP in Oakes Bay West Lake. In particular, the onset of this zone is marked by the presence of a pale grey-beige laminated sedimentary matrix and a sudden increase in the species *Asterionella formosa* (Figure 4). According to many geoarchaeological studies in Northeastern Canada and Greenland, the beginning of this period coincides with important cultural transitions and the short intervals of mild climatic conditions known as the Roman Warm Period (RWP) and the Medieval Warm Period (MWP).

Asterionella formosa is a species commonly associated with blooms following nutrient enrichment and anthropogenic atmospheric nitrogen deposition in recent sediments [83]. In the absence of these enrichments, its abundance, as well as other planktonic pennate diatoms such as *Fragilaria tenera* has been linked to increased air temperatures and consequent changes in the duration of open-water periods, thermal properties, and water column mixing regimes [83,84,101]. The elongate shape of this species (surface-to-volume ratio) and its ability to form stellate colonies enables it, along with *Fragilaria tenera* and *Tabellaria flocculosa*, to significantly reduce its sinking rate. These characteristics give these taxa a competitive advantage to exploit limited nutrient and light resources near the thermocline during periods of pronounced water column stability or nutrient resuspension during spring/autumnal mixing [83,101]. The significant decline in *Aulacoseira* spp. and the rapid recovery of *Discostella stelligera* after ca. 1400 and until ca. 310 cal. yr BP (Figure 4) support the hypothesis of changes in water column stability and stratification patterns, nutrient dynamics, and/or light availability [80,102].

The punctual abundance of *Asterionella formosa* species in Oakes Bay West Lake sediments (Figure 4), beginning drastically around 1520–1400 cal. yr BP and gradually decreasing until ca. 640 cal. yr BP, coincides with marked changes in physicochemical profiles. While detrital elements increase rapidly following ca. 1520 cal. yr BP and gradually decrease until

ca. 310 cal. yr BP, peaks in magnetic susceptibility and significant decreases in water and organic matter contents occur in two main phases, between ca. 1520–980 cal. yr BP and 640–310 cal. yr BP (Figure 3). These characteristics, combined with the presence of a coarser and highly variable sedimentary matrix between ca. 1520 and 640 cal. yr BP, suggest sudden increases in sedimentary inputs in an initially more energetic transport process, followed by a less important interval of fine sedimentation persisting until ca. 310 cal. yr BP [103]. Although a soil detachment or landslide at the base of Zone 3 cannot be ruled out, this type of initial deposition has also often been associated with high-magnitude floods or runoff events [103]. The continued decrease in detrital elements and magnetic susceptibility after ca. 310 cal. yr BP (Figure 3) suggests a gradual decrease in terrigenous inputs, while the return of Zone 2 species and *Asterionella formosa* in the last two centimetres (ca. 160–80 cal. yr BP; 1790–1870 AD; Figure 4) indicates some reorganization of diatom assemblages that is coherent with the chronological framework of terrestrial disturbances proposed by Roy et al. [5].

The expansion of mosses in the littoral zone of Oakes Bay West Lake is evidenced by the increase in the epiphytic benthic diatoms *Frustulia* spp. after 1050 cal. yr BP and *Eunotia* spp. after 610 yr. cal. BP (Figure 4) [1,79,102]. This multiplication of habitats is consistent with the increased diversity observed in the uppermost centimetres of the core. These species, which are common in North America, prefer the circumneutral to slightly acidic-coloured waters of peatlands, rich in humic substances and higher DOC concentrations [104]. Our results are in agreement with major development of peatlands starting from 1600 yr BP on the Québec–Labrador Peninsula [28]. On Dog Island, the establishment of hygrophilous plants (*Larix laricina*) at the north end of Oakes Bay West Lake around 1140 cal. BP, associated with the lateral expansion of a bog, closely corresponds to the development of the acidophilic benthic diatom community [5]. Suggesting climatic and/or hydrological modifications, the beginning of the gradual paludification of the terraces on the north shore of Oakes Bay has been dated at 800 cal. yr BP [5].

Nevertheless, despite the higher-resolution analysis carried out on the last two centimetres of the core, the very low sedimentation rate and the insufficient precision of the radiocarbon dates do not make it possible to easily distinguish or reliably document the short climatic periods of the late Holocene, such as the MWP, LIA, as well, as the impacts of anthropogenic activities or modern warming of atmospheric temperatures.

5.2. Palaeogeographic Evolution of Evilik Lake

The succession of biostratigraphic assemblages and variations in sedimentological and geochemical profiles suggest important palaeogeographic changes in the history of Evilik Lake during the Late Holocene. The analyses allowed us to identify three main phases leading to the isolation of the lake, reflecting processes of glacio-isostatic rebound, marine regression, and subsequent coastal evolution of Evilik Bay.

5.2.1. Glacio-Marine Environment (ca. 3350–2700 cal. yr BP)

The basal sediments of Evilik core were deposited in a context of ongoing marine regression and glacio-isostatic rebound, while the lake was in regular contact with the sea. This initial phase occurs during a period of transition and significant environmental change, marking the onset of the Neoglacial cooling.

The extensive fragmentation of diatom frustules, the predominance of small, highly silicified poly-mesohalobian benthic species, as well as the very low initial concentration of diatoms, particularly between ca. 3350 and 3100 cal. yr BP, suggest very unstable conditions with sediment transport and reworking [105]. These features, along with low assemblage diversity, have been observed in other arctic coastal regions where they typically occur in shallow dynamic nearshore environments that are under the influence of tidal action and sea ice scouring [78,106]. Peaks in magnetic susceptibility, the coarse inorganic sedimentary matrix with gravels and pebbles, and the high detrital element values support these conclusions [78]. The greater proportion and co-variation of Ca/Ti and Sr/Ti suggest

a primarily biogenic source of calcium carbonates and, in conjunction with high Br values (Figure 6), indicate a marine-influenced environment [53,107].

The species present, which are mostly epipsammic and epiphytic (*Pseudostaurosira perminuta*, *Cocconeis* spp., small *Opephora* spp., *Planothidium hauckianum*) (Figure 7), are typical constituents of these marine and brackish nearshore environments of European coasts, the North Atlantic, Australia, and Africa and recognized for their broad ecological tolerances [66,68,105,106,108]. They are closely associated with intertidal zones, supralittoral areas, as well as shallow (<5 m) coastal backshore environments characterized by sparse vegetation and sandy inorganic substrates, with salinities between 5 and 30‰ and sufficient light for photosynthesis [66,105,106,108–110]. Considering this information, the initial interval between ca. 3350 and 2930 cal. yr BP appears to have been formed in a dynamic shallow, relatively sheltered nearshore bay environment with an open connection allowing for marine influence [106,111].

As glacial isostatic rebound progressed and relative sea level lowered, marine activity and influence became increasingly restricted. The latter part of Zone 1 (ca. 2930–2700 cal. yr BP), which is marked by the presence of euryhaline mesohalobian epipelic species (*Navicula salinarum* and *Navicula digitoradiata*) and the decrease in polyhalobian species (Figure 7), infers increasingly brackish conditions [105,106]. Biostratigraphic assemblages from this short period are generally associated with supratidal areas characterized by mineral substrates and sparse vegetation, especially low-energy microtidal environments that are frequently inundated or influenced by marine aerosols, such as salt marshes and coastal ponds [68,105,110]. The shift to an epipelic flora tolerant of large salinity amplitudes would, thus, indicate the transition to calmer brackish conditions, marked by decreased tidal influence and wave action [112]. This coincides with a gradual decrease in grain size and the presence of small, very fine black fragments (Figure 6), possibly of plant origin. This transition would represent the gradual emersion of the lake, which occurred at least ca. 3000–2700 years ago.

5.2.2. Isolation Process and Brackish Conditions (ca. 2700–1990 cal. yr BP)

This transitional zone of laminated sedimentation is marked by the loss of regular marine influence and was possibly deposited in a coastal (breached) lake or lagoon with restricted circulation as the sill separating the lake gradually closed [66]. The passage to a highly diverse heterogeneous flora consisting of predominantly epipelic euryhaline mesohalobian species, as well as the highly variable pattern of Br (Figure 6), reveal brackish conditions subject to large and frequent fluctuations in salinity [66,106].

Increased freshwater and terrigenous sediment inputs via precipitation or runoff, consistent with the initial increase in detrital elements during initial lake isolation process starting after ca. 2700 cal. yr BP, contributed to the gradual decrease in salinity and the development of assemblages adapted to the highly variable conditions [66,78,106]. *Navicula kariana* var. *frigida* is a species typical of coastal environments, widespread in the Arctic Ocean and known to be associated with sea ice [68,113]. The low but continuous presence of *Fragilariopsis* spp. taxa, characteristic of cold waters and marginal ice zones, as well as mesohalobian species of the genus *Thalassiosira* (Figure 7), support the hypothesis of continuous influxes of cold freshwater, while their proliferation is intimately linked to sea ice melt [68,92,113,114]. Other mesohalobian species of the genus *Navicula* (*salinarum*, *phyllepta*, *phylleptosoma*, *gregaria*), which were found in slightly brackish conditions following lake isolation in Northern Quebec as well as in salt ponds and marshes of the Beaufort Sea coast and the Northwestern US coast, confirm the decrease in salinity [66,106,110]. The presence of lightly silicified *Chaetoceros* spp. taxa found in marine and brackish coastal environments is also consistent with increased freshwater inputs that enhanced water column stratification in a low-energy environment [90].

Stratification of the water column during this transition period (ca. 2700–1990 cal. yr BP) may have led to a temporary decrease in oxygenation at depth. This is supported by the presence of a euryhaline diatom flora characteristic of brackish conditions, the black

and laminated character of the sediments, and the marked increase in iron and sulfur concentrations (Figures 6 and 7), which are found under anoxic conditions [53,78,111,115]. Water column stratification with dense saltwater trapped under freshwater can occur during isolation of a lake when the threshold prevents saltwater flow and marine influence is restricted [106,111,116]. Dark and black sediments in this context are generally associated with the presence of iron monosulfides, precursors to pyrite, which form as a result of limited sulfate reduction in brackish waters and decreased oxygen availability [116]. This process, either caused by meromictic conditions or occasional exchange with the sea, has been observed in several lake basin isolation studies in Norway and the Canadian Arctic [78,111,115,116].

Various evidence suggests that this period (ca. 2700–1990 cal. yr BP) was disrupted by intermittent events allowing marine waters to cross the lake's threshold, possibly during storm surges. A storm surge or period of intense marine activity may have resulted in the breakdown or increased permeability of the sedimentary barrier protecting the lake basin, favouring the influx of seawater by waves or sea spray [107]. The co-variance of multiple indicators of marine influence at ca. 2600 and between 2460 and 2390 cal. yr BP suggests pronounced changes in sedimentation regime and diatom flora that are consistent with occasional transgression of cold, rich marine water. The punctual increase in allochthonous marine planktonic species (*Thalassionema nitzschioides*, *Chaetoceros*, silicoflagellates, and Ebridians) and Br, coupled with a coarser sedimentary matrix comprising many gravels and a decrease in organic matter content (Figures 6 and 7), supports this hypothesis [107,115]. Because the lake is located between Evilik and Oakes bays, the low elevation of the local topography may have facilitated the occurrence of these inwash/spillover events, thereby prolonging the maintenance of brackish conditions and the isolation process [106].

Thalassionema nitzschioides is a common polyhalobian planktonic species in the North Atlantic and North Sea, often associated with the warmer, saltier waters of the North Atlantic Drift or alternatively with cold, nutrient-rich upwelling zones [66,92,114]. Intermittent overflows of salty, nutrient-rich marine water into coastal Evilik Lake could, thus, have contributed to higher surface water productivity [115]. The decline in detrital mineral content over time was likely affected by increased primary productivity in the lake and its watershed, as reflected by higher values of LOI and biogenic silica (Si/Ti) after ca. 2390 cal. yr BP (Figure 6), or by stabilization of surrounding soils.

5.2.3. Freshwater Conditions (ca. 1990 cal. yr BP–Present)

The gradual replacement of saltwater by freshwater in a low-energy environment favoured the development of aquatic macrophytes and, consequently, the transition to a diatom flora dominated by halophilous epiphytes tolerant of slightly brackish conditions (e.g., *Cocconeis placentula*, *Diatoma elongatum*, *Pseudostaurosira subsalina*) (Figure 7) between ca. 1990 and 1840 cal. yr BP [66,105,106]. *Diatoma elongatum* is typical of low-salinity environments, found in high-conductivity freshwaters and brackish coastal waters [109]. *Nitzschia valdestriata* is an epipelic species found in brackish coastal environments but also common in supratidal and non-saline environments [68]. The presence of *Pseudostaurosira subsalina* during this short interval, an indicator species for these transitions to freshwater, as well as *Cocconeis placentula*, found in shallow coastal freshwater and brackish environments, reflect the progressive decrease in salinity, while the increase in Mn/Fe (Figure 7) is evidence for the gradual replacement and dilution of deep saline waters [68,105,111].

Fully lacustrine conditions were established ca. 1840 cal. yr BP with organic sedimentation and the appearance of an oligohalobian-indifferent and halophobian diatom flora typical of high-latitude boreal lakes [117]. The abundance of small fragilarioids (*Pseudostaurosira elliptica*, *P. pseudoconstruens*, *P. brevistriata*, *Staurosira venter*, *Staurosirella pinnata*), all indifferent mesoeuryhaline oligohalobian species, has been identified as a marker of lake basin isolation following marine regression and glacial-isostatic rebound in various studies in arctic regions of Canada and Finland [78,106,109,117]. Present in low numbers since ca. 3100 cal. yr BP, they increase rapidly following ca. 1990 cal. yr BP (Figure 7). Their presence

as a pioneer species in northern environments, as well as in recently deglaciated lakes, is often attributed to their high tolerance to unstable environmental conditions [78,109,117]. The predominance of these species, together with epiphytes associated with moss development (*Hygroptera balfouriana*, *Stauroforma exiguiformis*), as well as planktonic (*Aulacoseira perglabra*) and epipsammic (*Psammothidium* spp.) species, suggests a shift to circumneutral and slightly acidic oligotrophic freshwater conditions, the development of littoral habitats, and limnological stability over the last 1900 years [31,70].

5.3. Relative Sea Level Curves, Climate Changes, and Archaeological Implications

Oakes Bay West and Evilik lakes have provided valuable and complementary palaeogeographic information (Figure 8). In fact, while Evilik Lake (14 m asl) provided new data on the isostatic uplift and emersion of lands that would have been available for human occupation, Oakes Bay West Lake (40 m asl), isolated from the sea before 4900 cal. yr BP, informed us about both climate change and anthropogenic impacts on its watershed.

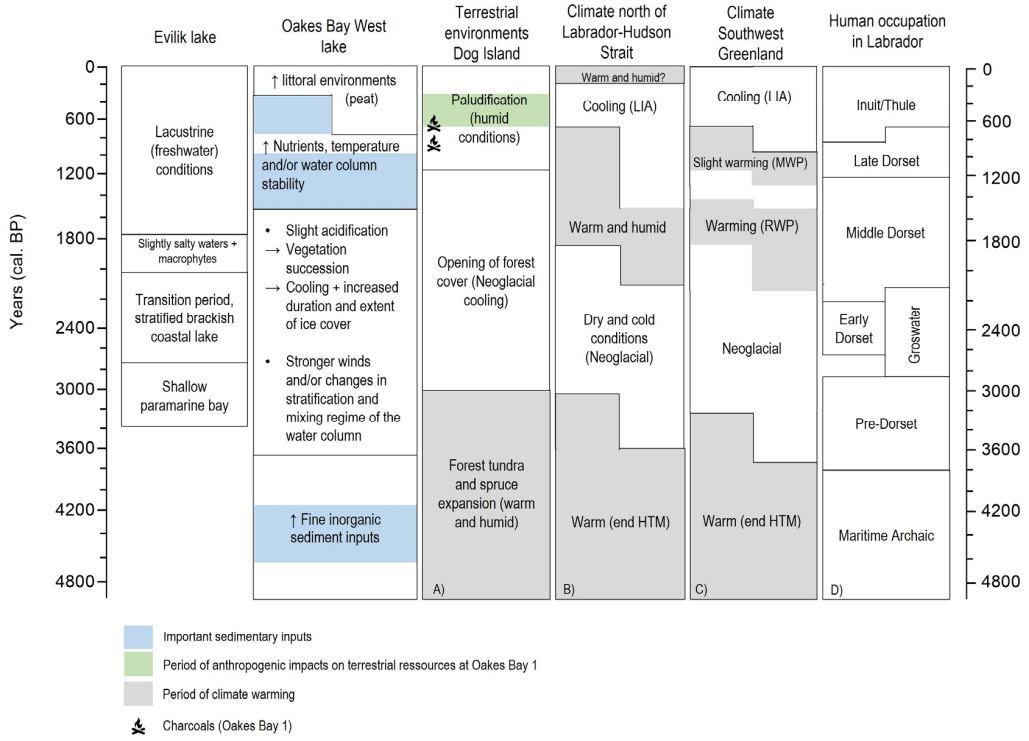

Figure 8. Key results from Oakes Bay West and Evilik lake cores in comparison to (**A**) the evolution of Dog Island terrestrial landscape [5], (**B**) palaeoclimatic conditions in northern Labrador and Hudson Strait [6,93,94,118,119], (**C**) palaeoclimatic conditions in southwestern Greenland [89,90,92,95], and (**D**) human occupation in Labrador [6,15]. Abbreviations: LIA—Little Ice Age, HTM—Holocene Thermal Maximum, RWM—Roman Warm Period, MWP—Medieval Warm Period.

In addition to climate and geophysical processes, anthropogenic activities may also have played a role in the changes observed in physicochemical parameters and diatom flora of Oakes Bay West Lake. For example, on Koliktalik Island, about 6 km east of Dog Island, charcoals were found in a peat monolith recovered from the Koliktalik 6 archaeological site (Figure 1) and dated to ca. 1650 cal. yr BP and ca. 540 cal. yr BP [5]. Accompanied by bone fragments, these were associated with human presence during two occupation phases, a first one during the Middle Dorset (2200–1200 cal. yr BP) and a second Thule/Inuit (13–15th to 17–18th centuries) [5]. On Dog Island, charcoals of anthropogenic origin have been identified in peat monoliths recovered near the Oakes Bay 1 archaeological site and dated to ca. 820 and 610 cal. yr BP [5]. Moreover, Inuit wood resource use between ca. 610 and 300 cal. yr BP, as highlighted by Roy et al. [5], had considerable impacts on the terrestrial

landscape of Dog Island. As human occupation is evident in the Dog Island area during this period [4,5,10,15,20], the combined influence of anthropogenic activities and associated disturbances in the watershed, climate, and geophysical processes on the physicochemical properties of the lake, including nutrient loading and additional export of sedimentary material, cannot be ruled out. Recently, Roy et al. [35] demonstrated that signs of human exploitation of forests around Nain and throughout its archipelago date as far back as the 17th century [5]. The increase in *Asterionella formosa* species we noted (Figure 7) has also previously been associated with human disturbances, including deforestation activities, which promote the export of nutrients (phosphorus, DOC) to lakes [120,121]. A study in the Canadian Arctic Archipelago (Somerset Island) also revealed the impacts of Thule whaling activities between 1200 and 1600 AD (750–350 cal. yr BP) on the ecosystemic integrity of lakes in the vicinity of former winter settlement sites, which resulted in increased nutrients and higher $\delta^{15}N$ ratios, extensive moss growth, and development of an epiphytic diatom flora [122].

Evilik Lake lies in a depression surrounded by geophysical barriers that isolate it from marine water from the island's two main bays. To the west, a long (~300 m) topographically constrained corridor ends at an elevation of 25 m asl and separates the lake from Oakes Bay. To the east, Evilik Bay is accessible at two main points and is located ~300 and ~500 m from the lake. The maximum elevation the sea would have to rise to reach the lake is 20 m asl to the northeast and 11–12 m asl to the east. Thus, we estimate that the lake may have been in contact with the sea as long as its level was >12 m.

Biostratigraphic, litho-sedimentological, and geochemical data show no evidence of erosion and suggest a gradual and prolonged isolation process starting around 3000–2700 cal. yr BP, corresponding to the loss of regular contact with the sea. Our results, however, assume a relatively closed-bay landscape since at least ca. 3350 cal. yr BP (2σ: 3056–3768 cal. yr BP), which would likely not have precluded human occupation on the elevated lake shore and would have been a possible attractive site due to its proximity to marine harvesting resources [13]. The minimum date of isolation proposed in this study, while much younger than the 5000–5500 yr BP (ca. 6000 cal. yr BP) age suggested by available relative sea level evolution curves for this elevation [22,23], is not in complete disagreement with the archaeological site dates documented and incorporated into the emersion curve by Clark and Fitzhugh [22] and the human occupation patterns in this region.

Charcoals from three nearby archaeological sites at a similar elevation to Evilik Lake, Thalia Point (10.6 and 11.7 m asl) and Nain (Quest Cove 1; 11.5 m asl), are dated, respectively, at 3597.5 ± 220.5, 3981 ± 247, and 4156.5 ± 253.5 cal. yr BP [23]. Charcoal recovered from a Dog Island site located at a slightly lower elevation (8.5 m asl), meanwhile, reveals a date of 2680 ± 70 yr BP (ca. 2803 cal. yr BP), while two higher sites (22.8 m asl) suggest much older ages of 6907 ± 233 and 7021 ± 232 cal. yr BP [22,23,25]. Integration and superposition of our results into the curves developed by Clark and Fitzhugh [22] for the Nain region and Vacchi et al. [23] for the north-central Labrador coast deflects these upward, suggesting either a slightly faster rate of isostatic rebound than previously estimated and a sea level that reached a plateau and remained stable for some period, or that some dates are inherently minimal or erroneous.

Despite the uncertainties associated with dating bulk organic sediments and extrapolation of lower-level dates, our reconstruction provides additional information on the glacial-isostatic rebound and relative sea level data for the Nain region. It, thereby, contributes to the interpretation of observed changes in settlement patterns over time, as landscape changes driven by coastal palaeogeographic evolution and relative sea level position likely influenced human communities establishing themselves in the Nain Archipelago, with impacts on available land, proximity to the sea, and accessibility of marine resources [13]. The decline in relative sea level, combined with land emersion and the formation of new terraces, may partially explain the abandonment and movement of settlements locations based on their proximity to the sea [13].

6. Conclusions

Analysis of diatom assemblages and physicochemical profiles preserved in the sediment cores of Oakes Bay West and Evilik lakes have allowed for a qualitative reconstruction of the late-Holocene environmental and climatic evolution of Dog Island, on the subarctic coast of Labrador. Although they exhibit different ecological changes and trajectories given the specific properties of their watershed topography, geographic location, limnological properties, and morphological characteristics, both study sites provided complementary data on the climate and environmental history of Dog Island. The results help to answer fundamental questions regarding how human societies have adapted in the context of Holocene climate fluctuations and changes in site habitability and resource proximity, as well as the impacts of climate variations, landscape evolution, and anthropogenic pressures on coastal subarctic lake ecosystems.

Results of Oakes Bay West Lake revealed additional information on the ecological and climate history of Dog Island since ca. 4900 cal. yr BP, as changes observed were closely linked to shifts in the watershed regarding vegetation cover, hydrological regimes (runoff, precipitation), geophysical factors (earthquakes, slope movement, etc.), and possible human disturbances, in addition to major climate fluctuations. The palaeolimnological evidence from Evilik Lake documented the sequence of isolation of the lake by the succession of polyhalobic, mesohalobic, and oligohalobic species, which allowed us to clarify the nature and chronology of the glacio-isostatic rebound, the marine regression, and the subsequent evolution of the coastline of Dog Island and availability of lands in the vicinity of archaeological sites.

However, given the low sediment accumulation and chronological resolution within the upper core levels, based on extrapolation of radiocarbon dates, our analyses could not accurately address the recent evolution of these ecosystems in the context of the MWP, LIA, and recent anthropogenic industrial-era warming. Several palaeoenvironmental studies conducted in high-latitude regions underscore the limitations imposed by low accumulation rates and the challenge of establishing reliable chronologies [77]. Dating of the upper levels should help adjust the chronological framework of the present study. Additional high-resolution research with a focus on lakes of the Labrador–Quebec Peninsula will help clarify certain questions and assumptions about the long-term ecological trajectory and vulnerability of coastal subarctic lakes, how landscape changes might have influenced human societies, and fill gaps regarding the emersion of lands and their subsequent occupation by humans.

Supplementary Materials: The following supporting information can be downloaded at: https://www.mdpi.com/article/10.3390/geosciences13040097/s1, Figure S1: PCA biplot of physicochemical data of Oakes Bay West Lake, Figure S2: PCA biplot of physicochemical data of Evilik Lake.

Author Contributions: C.L.-V.: Investigation, formal analysis, writing—original draft preparation; R.P.: Conceptualization, funding acquisition, resources, supervision, writing—review and editing; N.B.: writing—review and editing. All authors have read and agreed to the published version of the manuscript.

Funding: This research was funded by Fonds de recherche du Québec—Nature et technologies (FRQNT) grant number 274071, Northern Scientific Training Program (NSTP; Department of Indian and Northern Affairs), the Natural Sciences and Engineering Research Council of Canada (NSERC) grant numbers RGPIN-2020-06699 and 2017-04743 and the InterArctic (ANR-17-CE03-0009). Logistic and material support was provided by the Laboratoire de paléoécologie aquatique and Centre d'études nordiques (CEN), Université Laval.

Data Availability Statement: Data are contained within the article.

Acknowledgments: We thank L. Millet and D. Rius (Laboratoire Chrono-Environnement, UMR 6249 Centre national de la recherche scientifique, Université de Franche-Comté) for their contribution to geochemical analyses and field work, as well as D. Muir and X. Wang (Environment Canada, Burlington, Ontario) for water chemistry analyses and N. Roy (Geotop, Université du Québec à

Montréal). We thank our colleague James Woollett for many exchanges on the archaeoology of Labrador and to the Webb family for its collaboration. We are grateful to the village of Nain, its inhabitants for welcoming us and supporting our research, and to the reviewers of this manuscript.

Conflicts of Interest: The authors declare no conflict of interest. The funders had no role in the design of the study; in the collection, analyses, or interpretation of data; in the writing of the manuscript; or in the decision to publish the results.

References

1. Smol, J.P.; Wolfe, A.P.; Birks, J.B.; Douglas, M.S.V.; Jones, V.J.; Korhola, A.; Pienitz, R.; Rühland, K.; Sorvari, S.; Antoniades, D.; et al. Climate-driven regime shifts in the biological communities of arctic lakes. *Proc. Natl. Acad. Sci. USA* **2005**, *102*, 4397–4402. [CrossRef]
2. Brown, R.; Lemay, M. Variabilité et changements climatiques dans la péninsule du Nunavik et du Nunatsiavut (IRIS de la région subarctique de l'Est du Canada). In *De la Science aux Politiques Publiques. Une Étude Intégrée D'impact Régional des Changements Climatiques et de la Modernisation*; Allard, M., Lemay, M., Eds.; ArcticNet Inc.: Québec, QC, Canada, 2013; 318p.
3. Finnis, J.; Bell, T. An analysis of recent observed climate trends and variability in Labrador. *Can. Geogr. Geogr. Can.* **2015**, *59*, 151–166. [CrossRef]
4. Woollett, J. Oakes Bay 1: A Preliminary Reconstruction of a Labrador Inuit Seal Hunting Economy in the Context of Climate Change. *Geogr. Tidsskr. Dan. J. Geogr.* **2010**, *110*, 245–259. [CrossRef]
5. Roy, N.; Bhiry, N.; Woollett, J. Environmental Change and Terrestrial Resource Use by the Thule and Inuit of Labrador, Canada. *Geoarchaeology* **2012**, *27*, 18–33. [CrossRef]
6. Roy, N.; Woollett, J.; Bhiry, N. Paleoecological perspectives on landscape history and anthropogenic impacts at Uivak Point, Labrador, since AD 1400. *Holocene* **2015**, *25*, 1742–1755. [CrossRef]
7. Roy, N.; Bhiry, N.; Woollett, J.; Delwaide, A. A 550-Year Record of the Disturbance History of White Spruce Forests Near Two Inuit Settlements in Labrador, Canada. *J. North Atl.* **2017**, *16*, 1–14. [CrossRef]
8. Rosol, R.; Powell-Hellyer, S.; Man Chan, H. Impacts of decline harvest of country food on nutrient intake among Inuit in Arctic Canada: Impact of climate change and possible adaptation plan. *Int. J. Circumpolar Health* **2016**, *75*, 31127. [CrossRef] [PubMed]
9. Pienitz, R.; Douglas, M.S.V.; Smol, J.P. Paleolimnological research in polar regions: An introduction. In *Long-Term Environmental Change in Arctic and Antarctic Lakes*; Pienitz, R., Douglas, M.S.V., Smol, J.P., Eds.; Springer: Dordrecht, The Netherlands, 2004; pp. 1–17.
10. Sawada, M.; Gajewski, K.; de Vernal, A.; Richard, P. Comparison of marine and terrestrial Holocene climatic reconstructions from northeastern North America. *Holocene* **1999**, *9*, 267–277. [CrossRef]
11. Kaplan, M.R.; Wolfe, A.O. Spatial and temporal variability of Holocene temperature in the North Atlantic region. *Quat. Res.* **2006**, *65*, 223–231. [CrossRef]
12. Smol, J.P.; Cumming, B.F. Tracking long-term changes in climate using algal indicators in lake sediments. *J. Phycol.* **2000**, *36*, 986–1011. [CrossRef]
13. Fitzhugh, W. *Environmental Archeology and Cultural Systems in Hamilton Inlet, Labrador: A Survey of the Central Labrador Coast from 3000 B.C. to the Present*; Smithsonian Institution Press: Washington, WA, USA, 1972; 299p.
14. D'Andrea, W.J.; Huang, Y.; Fritz, S.C.; Anderson, N.J. Abrupt Holocene climate change as an important factor for human migration in West Greenland. *Proc. Natl. Acad. Sci. USA* **2011**, *108*, 9765–9769. [CrossRef] [PubMed]
15. Fitzhugh, W. Population movement and culture change on the central Labrador coast. *Ann. N. Y. Acad. Sci.* **1977**, *288*, 481–497. [CrossRef]
16. NICH-Arctic. Available online: http://nicharctic.ca/about/ (accessed on 2 December 2022).
17. Schledermann, P. The Effect of Climatic/Ecological Changes on the Style of Thule Culture Winter Dwellings. *Arct. Alp. Res.* **1976**, *8*, 37–47. [CrossRef]
18. Barry, R.G.; Arundale, W.H.; Andrews, J.T.; Nichols, H.; Bradley, R.S. Environmental Change and Cultural Change in the Eastern Canadian Arctic during the Last 5000 Years. *Arct. Alp. Res.* **1977**, *9*, 193–210. [CrossRef]
19. Woollett, J. Labrador Inuit subsistence in the context of environmental change: An initial landscape history perspective. *Am. Anthropol.* **2007**, *109*, 69–84. [CrossRef]
20. Couture, A.; Bhiry, N.; Monette, Y.; Woollett, J. A geochemical analysis of 18thcentury Inuit communal house floors in northern Labrador. *J. Archaeol. Sci. Rep.* **2016**, *6*, 71–81. [CrossRef]
21. Foury, Y. Inuit Winter Settlement Occupation at Oakes Bay 1, (HeCg-08), Labrador, Canada: Micromorphology and Zooarchaeology of Waste Disposal Sites. Master's Thesis, Université Laval, Quebec, QC, Canada, 2017.
22. Clark, P.U.; Fitzhugh, W. Late Deglaciation of the Central Labrador Coast and Its Implication for the Age of Glacial Lakes Naskaupi and McLean and for Prehistory. *Quat. Res.* **1990**, *34*, 296–305. [CrossRef]
23. Vacchi, M.; Engelhart, S.E.; Nikitina, D.; Ashe, E.L.; Peltier, R.W.; Roy, K.; Kopp, R.E.; Horton, B.P. Postglacial relative sea-level histories along the eastern Canadian coastline. *Quat. Sci. Rev.* **2018**, *201*, 124–146. [CrossRef]
24. AMS Dating Wood. Available online: https://www.radiocarbon.com/amsdating-wood.htm (accessed on 24 July 2022).
25. Canadian Archaeological Radiocarbon Database (CARD 2.1). Available online: http://www.canadianarchaeology.ca (accessed on 24 July 2022).

26. d'Arrigo, R.; Buckley, B.; Kaplan, S.; Woollett, J. Interannual to multidecadal modes of Labrador climate variability inferred from tree rings. *Clim. Dyn.* **2003**, *20*, 219–228. [CrossRef]
27. Richerol, T.; Fréchette, B.; Rochon, A.; Pienitz, R. Holocene climate history of the Nunatsiavut (northern Labrador, Canada) established from pollen and dinoflagellate cyst assemblages covering the past 7000 years. *Holocene* **2016**, *26*, 44–60. [CrossRef]
28. Short, S.K.; Nichols, H. Holocene Pollen Diagrams from Subarctic Labrador Ungava: Vegetanional History and Climatic Change. *Arct. Antarct. Alp. Res.* **1977**, *9*, 265–290. [CrossRef]
29. Lamb, H.F. Palynological Evidence for Postglacial Change in the Position of Tree Limit in Labrador. *Ecol. Monogr.* **1985**, *55*, 241–258. [CrossRef]
30. Levac, E.; de Vernal, A. Postglacial changes of terrestrial and marine environments along the Labrador coast: Palynological evidence from cores 91-045-005 and 91-045-006, Cartwright Saddle. *Can. J. Earth Sci.* **1997**, *34*, 1358–1365. [CrossRef]
31. Fallu, M.-A.; Pienitz, R.; Walker, I.R.; Lavoie, M. Paleolimnology of a shrub-tundra lake and response of aquatic and terrestrial indicators to climatic change in arctic Québec, Canada. *Palaeogeogr. Palaeoclimatol. Palaeoecol.* **2005**, *215*, 183–203. [CrossRef]
32. Saulnier-Talbot, É.; Larocque-Tobler, I.; Gregory-Eaves, I.; Pienitz, R. Response of lacustrine biota to late Holocene climate and environmental conditions in northernmost Ungava (Canada). *Arctic* **2015**, *68*, 153–168. [CrossRef]
33. Laing, T.E.; Pienitz, R.; Payette, S. Evaluation of Limnological Responses to Recent Environmental Change and Caribou Activity in the Riviere George Region, Northern Quebec, Canada. *Arct. Antarct. Alp. Res.* **2002**, *34*, 454–464. [CrossRef]
34. Richerol, T.; Pienitz, R.; Rochon, A. Recent anthropogenic and climatic history of Nunatsiavut fjords (Labrador, Canada). *Paleoceanography* **2014**, *29*, 869–892. [CrossRef]
35. Roy, N.; Woollett, J.; Bhiry, N.; Lemus-Lauzon, I.; Delwaide, A.; Marguerie, D. Anthropogenic and climate impacts on subarctic forests in the Nain region, Nunatsiavut: Dendroecological and historical approaches. *Ecoscience* **2021**, *28*, 361–376. [CrossRef]
36. Lemus-Lauzon, I.; Woollett, J.; Bhiry, N. Napâttuit: Wood use by Labrador Inuit and its impact on the forest landscape. *Inuit Stud.* **2012**, *36*, 113–137. [CrossRef]
37. Lemus-Lauzon, I.; Bhiry, N.; Woollett, J. Assessing the effects of climate change and land use on northern Labrador forest stands based on paleoecological data. *Quat. Res.* **2016**, *86*, 260–270. [CrossRef]
38. Wheeler, E.P., 2nd. The Nain. Okak Section of Labrador. *Geogr. Rev.* **1935**, *25*, 240–254. [CrossRef]
39. Ullah, W.; Beersing, A.; Blouin, A.; Wood, C.H.; Rodgers, A. *Water Resources Atlas of Newfoundland*; Water Resources Division, Department of Environment and Lands, Government of Newfoundland and Labrador: St John's, NL, Canada, 1992; pp. ii–80.
40. Macdonald, G.M. Some Holocene palaeoclimatic and palaeoenvironmental perspectives on Arctic/Subarctic climate warming and the IPCC 4th Assessment Report. *J. Quat. Sci.* **2010**, *25*, 39–47. [CrossRef]
41. Gibb, O.; Steinhauer, S.; Fréchette, B.; de Vernal, A.; Hillaire-Marcel, C. Diachronous evolution of sea surface conditions in the Labrador Sea and Baffin Bay since the last deglaciation. *Holocene* **2015**, *25*, 1882–1897. [CrossRef]
42. Données Climatiques Historiques. Available online: https://climat.meteo.gc.ca/ (accessed on 16 July 2022).
43. Payette, S.; Fortin, M.; Gamache, I. The subarctic forest-tundra: The structure of a biome in a changing climate. *Bioscience* **2001**, *51*, 709–718. [CrossRef]
44. Lemus-Lauzon, I.; Bhiry, N.; Arseneault, D.; Woollett, J.; Delwaide, A. Tree-ring evidence of changes in the subarctic forest cover linked to human disturbance in northern Labrador (Canada). *Écoscience* **2018**, *50*, 135–151. [CrossRef]
45. Blaauw, M.; Christen, J.A. rbacon: Age-Depth Modelling Using Bayesian Statistics. R Package Version 2.5.7. Available online: https://cran.rproject.org/web/packages/rbacon/index.html (accessed on 14 January 2021).
46. Blaauw, M.; Christen, J.A. Flexible paleoclimate age-depth models using an autoregressive gamma process. *Bayesian Anal.* **2011**, *6*, 457–474. [CrossRef]
47. Trachsel, M.; Telford, R.J. All age–depth models are wrong, but are getting better. *Holocene* **2016**, *27*, 860–869. [CrossRef]
48. Heiri, O.; Lotter, A.F.; Lemcke, G. Loss on ignition as a method for estimating organic and carbonate content in sediments: Reproducibility and comparability of results. *J. Paleolimnol.* **2001**, *25*, 101–110. [CrossRef]
49. Blott, S.J.; Pye, K. GRADISTAT: A grain size distribution and statistics package for the analysis of unconsolidated sediments. *Earth Surf. Process. Landf.* **2001**, *26*, 1237–1248. [CrossRef]
50. Richter, T.O.; Van der Gaast, S.; Koster, B.; Vaars, A.; Gieles, R.; de Stigter, H.C.; de Haas, H.; van Weering, T.C.E. The Avaatech XRF Core Scanner: Technical description and applications to NE Atlantic sediments. In *New Techniques in Sediment Core Analysis*; Rothwell, R.G., Ed.; Geological Society: London, UK, 2006; Special Publication 267; pp. 39–50.
51. Weltje, G.J.; Tjallingii, R. Calibration of XRF core scanners for quantitative geochemical logging of sediment cores: Theory and application. *Earth Planet. Sci. Lett.* **2008**, *274*, 423–438. [CrossRef]
52. Davies, S.J.; Lamb, H.F.; Roberts, S.J. Micro-XRF Core Scanning in Palaeolimnology: Recent Developments. In *Developments in Paleoenvironmental Research: Micro-XRF Studies of Sediment Cores*; Croudace, I.W., Rothwell, R.G., Eds.; Springer: Dordrecht, The Netherlands, 2015; Volume 17, pp. 189–226.
53. Rothwell, R.G.; Croudace, I.W. Twenty Years of XRF Core Scanning Marine Sediments: What Do Geochemical Proxies Tell Us? In *Micro-XRF Studies of Sediment Cores. Developments in Paleoenvironmental Research*; Croudace, I.W., Rothwell, R.G., Eds.; Springer: Dordrecht, The Netherlands, 2015; Volume 3, pp. 25–102.
54. Rioja: Analysis of Quaternary Science Data. R Package Version 0.9-21. Available online: https://cran.r-project.org/web/packages/rioja/index.html (accessed on 9 July 2021).

55. Vegan: Community Ecology Package. R Package Version 2.5-7. Available online: https://cran.r-project.org/web/packages/vegan/index.html (accessed on 9 July 2021).
56. Borcard, D.; Gillet, F.; Legendre, P. *Numerical Ecology with R*; Springer International Publishing: Cham, Germany, 2018; 435p.
57. Scherer, R. A new method for the determination of absolute abundance of diatoms and other silt-sized sedimentary particles. *J. Paleolimnol.* **1994**, *12*, 171–179. [CrossRef]
58. Battarbee, R.W.; Kneen, M.J. The use of electronically counted microspheres in absolute diatom analysis. *Limnol. Oceanogr.* **1982**, *27*, 184–188. [CrossRef]
59. Krammer, K. The genus Pinnularia. In *Diatoms of Europe—Diatoms of the European Inland Waters and Comparable Habitats*; Lange-Bertalot, H., Ed.; A.R.G. Gantner Verlag, K.G.: Ruggell, Liechtenstein, 2000; Volume 1, 703p.
60. Krammer, K. Cymbella. In *Diatoms of Europe—Diatoms of the European Inland Waters and Comparable Habitats*; Lange- Bertalot, H., Ed.; A.R.G. Gantner Verlag, K.G.: Ruggell, Liechtenstein, 2002; Volume 3, 584p.
61. Krammer, K. Cymbopleura, Delicata, Navicymbula, Gomphocymbellopsis, Afrocymbella. In *Diatoms of Europe—Diatoms of the European Inland Waters and Comparable Habitats*; Lange-Bertalot, H., Ed.; A.R.G. Gantner Verlag, K.G.: Ruggell, Liechtenstein, 2003; Volume 4, 530p.
62. Krammer, K.; Lange-Bertalot, H. Bacillariophyceae 1. Teil: Naviculaceae. In *Süßwasserflora von Mitteleuropa*; Ettl, H., Gerloff, J., Heynig, H., Mollenhauer, D., Eds.; Gustav Fischer Verlag: Stuttgart, Germany; New York, NY, USA, 1986; 876p.
63. Krammer, K.; Lange-Bertalot, H. Bacillariophyceae 2. Teil: Bacillariaceae, Epithemiaceae, Surirellaceae. In *Süßwasserflora von Mitteleuropa*; Ettl, H., Gerloff, J., Heynig, H., Mollenhauer, D., Eds.; Gustav Fischer Verlag: Stuttgart, Germany; New York, NY, USA, 1988; 596p.
64. Krammer, K.; Lange-Bertalot, H. Bacillariophyceae 3. Teil: Centrales, Fragilariaceae, Eunotiaceae. In *Süßwasserflora von Mitteleuropa*; Ettl, H., Gerloff, J., Heynig, H., Mollenhauer, D., Eds.; Gustav Fischer Verlag: Stuttgart, Germany; New York, NY, USA, 1991; 576p.
65. Krammer, K.; Lange-Bertalot, H. Bacillariophyceae 4. Bacillariophyceae 4. Teil: Achnanthaceae, Kritische Ergänzungen zu Navicula (Lineolatae) und Gomphonema. In *Süßwasserflora von Mitteleuropa*; Ettl, H., Gerloff, J., Heynig, H., Mollenhauer, D., Eds.; Gustav Fischer Verlag: Stuttgart, Germany; Jena, Germany, 1991; 473p.
66. Campeau, S.; Pienitz, R.; Héquette, A. *Diatoms from the Beaufort Sea Coast, Southern Arctic-Ocean (Canada). Modern Analogues for Reconstructing Late Quaternary Environments and Relative Sea Levels*; Cramer: Stuttgart, Germany, 1999; Bibliotheca Diatomologica; Volume 42, 244p.
67. Fallu, M.-A.; Allaire, N.; Pienitz, R. *Freshwater Diatoms from Northern Québec and Labrador (Canada). Species-Environment Relationships in Lakes of Boreal Forest, Forest-Tundra and Tundra Regions*; Cramer: Stuttgart, Germany, 2000; Bibliotheca Diatomologica; Volume 45, 200p.
68. Witkowski, A.; Lange-Bertalot, H.; Metzeltin, D. *Diatom Flora of Marine Coasts*; A.R.G. Gantner Verlag: Ruggell, Liechtenstein, 2000; Iconographia Diatomologica; Volume 7, 925p.
69. Lange-Bertalot, H. Navicula sensu stricto, 10 genera separated from Navicula sensu lato, Frustulia. In *Diatoms of Europe—Diatoms of the 90 European Inland Waters and Comparable Habitats*; Lange-Bertalot, H., Ed.; A.R.G. Gantner Verlag: Ruggell, Liechtenstein, 2001; Volume 2, 526p.
70. Antoniades, D.A.; Hamilton, P.B.; Douglas, M.S.V.; Smol, J.P. *Diatoms of North America: The Freshwater Floras of Prince Patrick, Ellef Ringnes and Northern Ellesmere Islands from the Canadian Arctic Archipelago*; A.R.G. Gantner Verlag: Ruggell, Liechtenstein, 2008; Iconographia Diatomologica; Volume 17, 649p.
71. Zimmermann, C.; Poulin, M.; Pienitz, R. *The Pliocene-Pleistocene Freshwater Flora of Bylot Island, Nunavut, Canadian High Arctic*; A.R.G. Gantner Verlag: Ruggell, Liechtenstein, 2010; Iconographia Diatomologica; Volume 21, 407p.
72. Lange-Bertalot, H.; Bak, M.; Witkowski, A. Eunotia and some related genera. In *Diatoms of Europe—Diatoms of the European Inland Waters and Comparable Habitats*; Lange-Bertalot, H., Ed.; A.R.G. Gantner Verlag: Ruggell, Liechtenstein, 2011; Volume 6, 747p.
73. Juggins, S. *Software for Ecological and Palaeoecological Data Analysis and Visualisation*; C2 Version 1.7.6; University of Newcastle upon Tyne: Newcastle upon Tyne, UK, 2014.
74. R Core Team. *R: A Language and Environment for Statistical Computing*; R Foundation for Statistical Computing Version 4.1.3: Vienna, Austria, 2022.
75. RStudio Team. *Rstudio: Integrated Development for R*; RStudio Version 2021.09.0+351, PBC: Boston, MA, USA, 2022.
76. Legendre, P.; Gallagher, E.D. Ecologically meaningful transformations for ordination of species data. *Oecologia* **2001**, *129*, 271–280. [CrossRef] [PubMed]
77. Saulnier-Talbot, É.; Pienitz, R.; Stafford, T.W. Establishing Holocene sediment core chronologies for northern Ungava lakes, Canada, using humic acids (AMS 14C) and 210Pb. *Quat. Geochronol.* **2009**, *4*, 278–287. [CrossRef]
78. Narancic, B.; Pienitz, R.; Chapligin, B.; Meyer, H.; Francus, P.; Guilbault, J.-P. Postglacial environmental succession of Nettilling Lake (Baffin Island, Canadian Arctic) inferred from biogeochemical and microfossil proxies. *Quat. Sci. Rev.* **2016**, *147*, 391–405. [CrossRef]
79. Pienitz, R.; Smol, J.P.; MacDonald, G.M. Paleolimnological reconstruction of holocene climatic trends from two boreal treeline lakes, Northwest Territories, Canada. *Arct. Antarct. Alp. Res.* **1999**, *31*, 82–93. [CrossRef]
80. Rühland, K.; Smol, J.P. Diatom shifts as evidence for recent Subarctic warming in a remote tundra lake, NWT, Canada. *Palaeogeogr. Palaeoclimatol. Palaeoecol.* **2005**, *226*, 1–16. [CrossRef]
81. Perren, B.B.; Douglas, M.S.V.; Anderson, N.J. Diatoms reveal complex spatial and temporal patterns of recent limnological change in West Greenland. *J. Paleolimnol.* **2008**, *42*, 233–247. [CrossRef]

82. Narancic, B.; Saulnier-Talbot, É.; St-Onge, G.; Pienitz, R. Diatom sedimentary assemblages and Holocene pH reconstruction from the Canadian Arctic Archipelago's largest lake. *Écoscience* **2021**, *28*, 347–360. [CrossRef]
83. Rühland, K.M.; Paterson, A.M.; Smol, J.P. Lake diatom responses to warming: Reviewing the evidence. *J. Paleolimnol.* **2015**, *54*, 1–35. [CrossRef]
84. Laing, T.E.; Pienitz, R.; Smol, J.P. Freshwater diatom assemblages from 23 lakes located near Norilsk, Siberia: A comparison with assemblages from other circumpolar treeline regions. *Diatom Res.* **1999**, *14*, 285–305. [CrossRef]
85. Engstrom, D.R.; Fritz, S.C.; Almendinger, J.E.; Juggins, S. Chemical and biological trends during lake evolution in recently deglaciated terrain. *Nature* **2000**, *408*, 161–166. [CrossRef]
86. Saulnier-Talbot, É.; Pienitz, R.; Vincent, W. Holocene Lake succession and palaeooptics of a Subarctic lake, northern Québec, Canada. *Holocene* **2003**, *13*, 517–526. [CrossRef]
87. Levac, E.; de Vernal, A.; Blake, W., Jr. Sea-surface conditions in northernmost Baffin Bay during the Holocene: Palynological evidence. *J. Quat. Sci.* **2001**, *16*, 353–363. [CrossRef]
88. Kaplan, M.R.; Wolfe, A.P.; Miller, G.H. Holocene environmental variability in southern Greenland inferred from lake sediments. *Quat. Res.* **2002**, *58*, 149–159. [CrossRef]
89. Møller, H.S.; Jensen, K.G.; Kuijpers, A.; Aagaard-Sørensen, S.; Seidenkrantz, M.-S.; Prins, M.; Endler, R.; Mikkelsen, N. Late-Holocene environment and climatic changes in Ameralik Fjord, southwest Greenland: Evidence from the sedimentary record. *Holocene* **2006**, *16*, 685–695. [CrossRef]
90. Moros, M.; Jensen, K.; Kuijpers, A. Mid- to late-Holocene hydrological and climatic variability in Disko Bugt, central west Greenland. *Holocene* **2006**, *16*, 357–367. [CrossRef]
91. Seidenkrantz, M.-S.; Aagaard-Sorensen, S.; Sulsbrueck, H.; Kuijpers, A.; Jensen, K.G.; Kunzendorf, H. Hydrography and climate of the last 4400 years in a SW Greenland fjord: Implications for Labrador Sea palaeoceanography. *Holocene* **2007**, *17*, 387–401. [CrossRef]
92. Sha, L.; Jiang, H.; Seidenkrantz, M.-S.; Knudsen, K.L.; Olsen, J.; Kuijpers, A.; Liu, Y. A diatom-based sea-ice reconstruction for the Vaigat Strait Disko Bugt, West Greenland over the last 5000 yr. *Palaeogeogr. Palaeoclimatol. Palaeoecol.* **2014**, *403*, 66–79. [CrossRef]
93. Kerwin, M.W.; Overpeck, J.T.; Webb, R.S.; Anderson, K.H. Pollen-based summer temperature reconstructions for the eastern Canadian boreal forest, subarctic, and Arctic. *Quat. Sci. Rev.* **2004**, *23*, 1901–1924. [CrossRef]
94. Lochte, A.A.; Repschläger, J.; Seidenkrantz, M.-S.; Kienast, M.; Blanz, T.; Schneider, R.R. Holocene water mass changes in the Labrador Current. *Holocene* **2019**, *29*, 676–690. [CrossRef]
95. Lloyd, J.M.; Kuijpers, A.; Long, A.; Moros, M.; Park, L.A. Foraminiferal reconstruction of mid to late-Holocene Ocean circulation and climate variability in Disko Bugt, West Greenland. *Holocene* **2007**, *17*, 1079–1091. [CrossRef]
96. Michelutti, N.; Wolfe, A.P.; Briner, J.P.; Miller, G.H. Climatically controlled chemical and biological development in Arctic lakes. *J. Geophys. Res.* **2007**, *112*, 1–10. [CrossRef]
97. Rühland, K.; Priesnitz, A.; Smol, J.P. Paleolimnological Evidence from Diatoms for Recent Environmental Changes in 50 Lakes across Canadian Arctic Treeline. *Arct. Antarct. Alp. Res.* **2003**, *35*, 110–123. [CrossRef]
98. Finkelstein, S.A.; Bunbury, J.; Gajewski, K.; Wolfe, A.P.; Adams, J.K.; Delvin, J.E. Evaluating diatom-derived Holocene pH reconstructions for Arctic lakes using an expanded 171-lake training set. *J. Quat. Sci.* **2014**, *29*, 249–260. [CrossRef]
99. Wolfe, A.P. Climate modulates the acidity of arctic lakes on millennial time scales. *Geology* **2002**, *30*, 215. [CrossRef]
100. Saros, J.E.; Anderson, N.J. The ecology of the planktonic diatom Cyclotella and its implications for global environmental change studies. *Biol. Rev.* **2015**, *90*, 522–541. [CrossRef]
101. Sivarajah, B.; Rühland, K.M.; Labaj, A.L.; Paterson, A.M.; Smol, J.P. Why is the relative abundance of *Asterionella formosa* increasing in a Boreal Shield lake as nutrient levels decline? *J. Paleolimnol.* **2016**, *55*, 357–367. [CrossRef]
102. Paull, T.M.; Finkelstein, S.A.; Gajewski, K. Interactions between climate and landscape drive Holocene ecological change in a High Arctic lake on Somerset Island, Nunavut, Canada. *Arct. Sci.* **2017**, *3*, 17–38. [CrossRef]
103. St-Onge, G.; Mulder, T.; Piper, D.J.W.; Hillaire-Marcel, C.; Stoner, J.S. Earthquake and flood-induced turbidities in the Saguenay Fjord (Québec): A Holocene paleoseismicity record. *Quat. Sci. Rev.* **2004**, *23*, 283–294. [CrossRef]
104. Pienitz, R. Analyse des microrestes végétaux: Diatomées. In *Écologie des Tourbières du Québec-Labrador*; Payette, S., Rochefort, L., Eds.; Les Presses de l'Université Laval: Quebec City, QC, Canada, 2001; pp. 311–326.
105. Vos, P.C.; de Wolf, H. Diatoms as a tool for reconstructing sedimentary environments in coastal wetlands; methodological aspects. *Hydrobiologia* **1993**, *269/270*, 285–296. [CrossRef]
106. Pienitz, R.; Lortie, G.; Allard, M. Isolation of Lacustrine Basins and Marine Regression in the Kuujjuaq Area, Northern Québec, as Inferred from Diatom Analysis. *Géographie Phys. Quat.* **1991**, *45*, 155–174. [CrossRef]
107. Oliva, F.; Peros, M.; Viau, A. A review of the spatial distribution of and analytical techniques used in paleotempestological studies in the western North Atlantic Basin. *Prog. Phys. Geogr.* **2017**, *41*, 171–190. [CrossRef]
108. Sabbe, K.; Vyverman, W. Taxonomy, morphology and ecology of some widespread representatives of the diatom genus Opephora. *Eur. J. Phycol.* **1995**, *30*, 235–249. [CrossRef]
109. Weckström, K.; Juggins, S. Coastal Diatom-Environment Relationships from the Gulf of Finland, Baltic Sea. *J. Phycol.* **2006**, *42*, 21–35. [CrossRef]
110. Sawai, Y.; Horton, B.P.; Kemp, A.C.; Hawkes, A.D.; Nagumo, T.; Nelson, A.R. Relationships between diatoms and tidal environments in Oregon and Washington, USA. *Diatom Res.* **2016**, *31*, 17–38. [CrossRef]

111. Cuven, S.; Francus, P.; Lamoureux, S. Mid to Late Holocene hydroclimatic and geochemical records from the varved sediments of East Lake, Cape Bounty, Canadian High Arctic. *Quat. Sci. Rev.* **2011**, *30*, 2651–2665. [CrossRef]
112. Denys, L. Diatom assemblages along a former intertidal gradient: A palaeoecological study of a subboreal clay layer (western coastal plain, Belgium). *Neth. J. Aquat. Ecol.* **1994**, *28*, 85–96. [CrossRef]
113. Pearce, C.; Weckström, K.; Sha, L.; Miettinen, A.; Seidenkrantz, M. The Holocene marine diatom flora of Eastern Newfoundland bays. *Diatom Res.* **2014**, *29*, 441–454. [CrossRef]
114. Oksman, M.; Juggins, S.; Miettinen, A.; Witkowski, A.; Weckström, K. The biogeography and ecology of common diatom species in the northern North Atlantic, and their implications for paleoceanographic reconstructions. *Mar. Micropaleontol.* **2019**, *148*, 1–28. [CrossRef]
115. Balascio, N.L.; Zhang, Z.; Bradley, R.S.; Perren, B.; Dahl, S.O.; Bakke, J. A multiproxy approach to assessing isolation basin stratigraphy from the Lofoten Islands, Norway. *Quat. Res.* **2011**, *75*, 288–300. [CrossRef]
116. Retelle, M.J.; Bradley, R.S.; Stuckenrath, R. Relative Sea Level Chronology Determined from Raised Marine Sediments and Coastal Isolation Basins, Northeastern Ellesmere Island, Arctic Canada. *Arct. Alp. Res.* **1989**, *21*, 113–125. [CrossRef]
117. Saulnier-Talbot, É.; Pienitz, R. Isolation au postglaciaire d'un bassin côtier près de Kuujjuaraapik-Whapmagoostui, en Hudsonie (Québec): Une analyse biostratigraphique diatomifère. *Géographie Phys. Quat.* **2001**, *55*, 63–74. [CrossRef]
118. Kasper, J.N.; Allard, M. Late-holocene climatic changes as detected by the growth and decay of ice wedges on the southern shore of Hudson strait, northern Québec, Canada. *Holocene* **2001**, *11*, 563–577. [CrossRef]
119. Ouzilleau Samson, D.; Bhiry, N.; Lavoie, M. Late-Holocene palaeoecology of a polygonal peatland on the south shore of Hudson Strait, northern Québec, Canada. *Holocene* **2010**, *20*, 525–536. [CrossRef]
120. Köster, D.; Pienitz, R.; Wolfe, B.B.; Barry, S.; Foster, D.R.; Dixit, S.S. Paleolimnological assessment of human-induced impacts on Walden Pond (Massachusetts, USA) using diatoms and stable isotopes. *Aquat. Ecosyst. Health Manag.* **2005**, *8*, 117–131. [CrossRef]
121. Hausmann, S.; Pienitz, R. Seasonal water chemistry and diatom changes in six boreal lakes of the Laurentian Mountains (Québec, canada): Impacts of climate and timber harvesting. *Hydrobiol. Int. J. Aquat. Sci.* **2009**, *635*, 1–14. [CrossRef]
122. Douglas, M.S.V.; Smol, J.P.; Savelle, J.M.; Blais, J.M. Prehistoric Inuit whalers affected arctic freshwater ecosystems. *Proc. Natl. Acad. Sci. USA* **2004**, *101*, 1613–1617. [CrossRef]